Journal of Controlled Release 324 (2020) 379–404

Contents lists available at ScienceDirect

Journal of Controlled Release

journal homepage: www.elsevier.com/locate/jconrel

Review article

Recent advances in long-acting nanoformulations for delivery of antiretroviral drugs

Dhanashree H. Surve, Anil B. Jindal*

Department of Pharmacy, Birla Institute of Technology and Science Pilani, Pilani Campus, Jhunjhunu, Rajasthan 333031, India

ARTICLE INFO

Keywords:
long-acting
in-vitro and *in-vivo* model
nanoprodrug and nanodrug
nanocrystal
aspherical nanoparticles
polymeric and lipidic nanoparticle

ABSTRACT

In spite of introduction of combination antiretroviral therapy (cART) against human immunodeficiency virus (HIV) infection; inaccessibility and poor adherence to oral cART costs 10 in 100,000 death worldwide. Failure in adherence leads to viral rebound, emergence of drug resistance and anticipated HIV infection in high risk individuals. Various Long-acting antiretroviral (LA ARV) nanoformulations including nano-prodrug, solid drug nanoparticles (SDN), nanocrystals, aspherical nanoparticles, polymeric and lipidic nanoparticles have shown plasma/tissue drug concentration in the therapeutic range for several weeks during pre-clinical evaluation. LA ARV nanoformulations therefore have replaced cART as better alternative for the treatment of HIV infection. Cabenuva™ is recently approved by Health Canada containing LA cabotegravir + LA rilpivirine nanocrystals (ViiV healthcare) for once monthly administration by intramuscular route. The LA nanoformulation due to its nanosize insist on better stability, delivery to lymphatic, slow release into systemic circulation via lymphatic-circulatory system conjoint and secondary drug depot within infiltered immune cells at site of administration and systemic circulation in contrast to conventional drugs. However, the pharmacokinetic, biodistribution and efficacy of LA nanoformulations hinge onto physicochemical properties of the drugs and route of administration. Therefore, current review emphasizes on these contradistinctive factors that affects the reproducibility, safety, efficacy and toxicity of LA anti-HIV nanoformulations. Moreover, it expatiates on application of profuse nanoformulations for long-acting effect with promising preclinical discoveries and two clinical leads. To add on, utilization of physiology-based and mechanism-based pharmacokinetic modelling and *in vivo* animal models which could lead to enhanced safety and efficacy of LA ARV nanoformulations in humans have been included.

1. Introduction

The advent of combination antiretroviral therapy (cART) in 1995 led to successful chronic management of human immunodeficiency virus (HIV) infection [1]. However, only 24.5 million people among 37.9 million HIV infected population were accessing cART by the end of June, 2019 [2,3]. Currently, there are 1.7 million children (< 15 years) [2] and 4.2 million older adults (> 50 years) [4] infected with HIV who are more prone to failure of treatment adherence due to the complexity of cART [5]. Almost ten deaths per 100,000 people all over the world

Abbreviations: AOT, 1,4-bis-(2-ethylhexoxy)-1,4-dioxybutane-2-sulfonate; API, Active pharmaceutical ingredient; ARV, Antiretroviral; ATLAS, Antiretroviral therapy as long acting suppression; ATV, Atazanavir; AUC, Area under curve; BLT, Bone marrow-liver-thymus; CAB LAP, Cabotegravir Long acting parenteral; cART, Combination antiretroviral therapy; C_{max}, Maximum concentration; DcNP, Combination drug nanoparticle; DKO, Double knock out; DSPC, Distearoyl phosphatidylcholine; DSPE, 1,2-distearoyl-sn- glycerol-3-phosphoethanolamine; EVG, Elvitegravir; FA nano ATV/r, folic acid-conjugated poloxamer 407 incorporating atazanavir boosted with ritonavir; FLAIR, First long acitng injectable regimen; FTC, Emtricitabine; GIT, Gastrointestinal tract; HIV, Human immunodeficiency virus; Hu PBL, Human peripheral blood mononuclear lymphocyte; HSPC, hematopoietic stem/progenitor cells; IM, Intramuscular; IV, Intravenous; LA, Long acting; LASER, Long acting slow effective release; LATTE, Long acting antiretroviral treatment enabling trial; LDN, Lipid drug nanoparticle; MAP, Microtubule associated protein; MBPK, Mechanism-based pharmacokinetic; MCAB, Myristoylated cabotegravir; MDM, Monocyte derived macrophage; MoM, Myeloid only mice; MRT, Mean residence time; M3RPV, Myristoylated rilpivirine; NCAB, Nanocrystal suspension of cabotegravir; NFTC, Nanocrystal suspension of emtricitabine; NHP, Non human primate; NMFTC, Nanosuspension of palmitoylated emtricitabine; NMCAB, Nanosuspension myristoylated cabotegravir; NM3RPV, Nanosuspension of myristoylated rilpivirine; NNRTI, Non-nucleoside reverse transcriptase inhibitor; NRTI, Nucleoside reverse transcriptase inhibitor; NOD, Non obese diabetic; PBPK, Physiology-based pharmacokinetic; PEG, Polyethylene glycol; PLGA, Poly-(lactic-co-glycolic acid); PVA, Polyvinyl alcohol; PSA, Polar surface area; SCID, Severe combined immunodeficiency; Thy/Liv, Thymus-Liver; TLC-ART-101, Targeted long-acting antiretroviral therapy product candidate 101

* Corresponding author.
E-mail address: anil.jindal@pilani.bits-pilani.ac.in (A.B. Jindal).

https://doi.org/10.1016/j.jconrel.2020.05.022
Received 27 April 2020; Received in revised form 14 May 2020; Accepted 15 May 2020
Available online 24 May 2020
0168-3659/ © 2020 Elsevier B.V. All rights reserved.

Table 1
Available oral cART against HIV-1 infection.

Sr. no	cART	Strength (mg)	Half-life (h)	Frequency of administration	References
Four drug combination					
1	Elvitegravir	150	9.9	One tablet, once daily	[27,28]
	Cobicistat	150	4.3		
	Emtricitabine	200	4.8		
	tenofovir AF	10	51.3		
2	Elvitegravir	150	9.9	One tablet, once daily	[27,29]
	cobicistat	150	4.3		
	emtricitabine	200	4.8		
	tenofovir DF	300	18.3		
3	Darunvir	800	14.6	One tablet, once daily	[27,30]
	cobicistat	150	4.3		
	emtricitabine	200	4.8		
	tenofovir AF	10	51.3		
Three drug combination					
4	Bictegravir	50	17.8	One tablet, once daily	[27,31]
	Emtricitabine	200	4.8		
	tenofovir alfanamide (AF)	25	51.3		
5	Efavirenz	600	37.7	One tablet, once daily	[27,32]
	Emtricitabine	200	4.8		
	tenofovir disproxil fumarate (DF)	300	18.3		
6	Rilpivirine	25	48	One tablet, once daily	[27,33]
	Emtricitabine	200	4.8		
	tenofovir DF	300	18.3		
7	Doravirine	100	15	One tablet, once daily	[27,34,35]
	lamivudine	300	5.4		
	tenofovir DF	300	18.3		
8	Rilpivirine	25	48	One tablet, once daily	[27,36]
	Emtricitabine	200	4.8		
	tenofovir AF	25	51.3		
9	Efavirenz	400	37.7	One tablet, once daily	[27,32]
	lamivudine	300	5.4		
	tenofovir DF	300	18.3		
10	Dolutegravir	50	13.5	One tablet, once daily	[37,38]
	abacavir	600	1.3		
	lamivudine	300	5.4		
11	Abacavir	300	1.3	One tablet, twice daily	[27,39]
	lamivudine	150	5.4		
	zidovudine	300	1.2		
Two drug combination					
12	Dolutegravir	50	13.5	One tablet, once daily	[27,40]
	Rilpivirine	25	48		
13	Lamivudine	300	5.4	One tablet, once daily	[27,41]
	tenofovir DF	300	18.3		
14	Lamivudine	150	5.4	One tablet, twice daily	[27,42]
	Zidovudine	300	1.2		
15	Emtricitabine	200	4.8	One tablet, once daily	[27,43]
	Tenofovir AF	25	51.3		
16	Abacavir	600	1.3	One tablet, once daily	[27,44]
	Lamivudine	300	5.4		
17	Emtricitabine	100/133/167/200	4.8	One tablet, once daily	[27,45]
	Tenofovir DF	150/200/250/300	18.3		
18	Atazanavir	300	7.5	One tablet, once daily	[27,46]
	Cobicistat	150	4.3		
19	Lopinavir	200/400	5-6	One tablet, twice daily (400 mg/100 mg)	[27,47,48]
	ritonavir	50/100	3.5	Or Two tablets, twice daily (200 mg, 50 mg) Or 5 ml solution containing 80 mg/ml and 20 mg/ml twice daily	
20	Darunavir	800	14.6	One tablet, once daily	[27,49]
	cobicistat	150	4.3		

[6] occur either due to lack of cART access or poor cART adherence. Failure in adherence leads to viral rebound and the emergence of drug resistance [7]. Further, persistent adherence of cART in patients with pre-exposure prophylaxis (PrEP) is desirable to reduce the risk of HIV infection [8]. Various cART are currently under clinical use with frequent dosing regimen for treatment of HIV and pre-exposure prophylaxis (Table 1). However, Long-acting antiretroviral (LA ARV) nanoformulation with weekly or monthly administration could be an irresistible approach to prevent the risks associated with HIV [9]. Intramuscular (IM) and subcutaneous (SC) sites have long been explored as depot deliverables. Therefore, IM or SC administration of long-acting (LA) nanoformulation could lead to the delivery of antiretroviral therapy (ART) into HIV residence and spread sites due to the presence of lymphatic vesicles at these sites [10]. Additionally, LA ARV

nanoformulation leads to the formation of the secondary depot in immune cells, which are infiltered at administration site [11] or tissue lymphocytes [12] causing week- or month-long sustained drug release. LA ARV nanoformulations further leads to steady plasma concentration within the therapeutic range with reduced dose and frequency of administration.

Various aspects of LA injectables, including rilpivirine and cabotegravir nanocrystal pharmacology [13,14] and potential leads for LA anti-retroviral injectables [15] were reviewed earlier. In addition, various platform technologies for LA drug delivery via both oral and parenteral route [16,17], challenges associated with each technology, mechanism of drug release and sustained plasma exposure from LA injectables [17] were also reviewed. The present review elaborates on the lacunae regarding physicochemical properties of drugs specifically suitable for LA ARV nanoformulation, effect of route of administration and involvement of circulatory-lymphatic system conjoint in LA slow effective release of ARV. More distinctly, successful clinical cabotegravir LA (GlaxoSmithKlein plc) and rilpivirine LA (Jannsen Pharmaceutical Inc.) nanocrystals individually and cabotegravir LA+ rilpivirine LA by ViiV healthcare has been narrated. To add on, promises and pitfalls associated with preclinical hits including nanocrystal and nanoprodrug, solid drug nanocarriers (SDN), polymeric and lipid nanocarriers incorporating single or combination antiretrovirals have been described. The application of *in vitro* [18–21] and *in vivo* models [22–26] to synthesize LA nanoformulation with efficient safety and efficacy in humans has also been included.

2. General considerations involved in the development of long-acting nanoformulations

2.1. Desired physicochemical and pharmacokinetic properties of active pharmaceutical ingredients for long-acting nanoformulations

The main objective of LA nanoformulations is to provide sustained drug release to achieve constant and effective plasma drug concentration at the desired site for weeks or months [17]. LA ARV nanoformulations for HIV prophylaxis and cure have been developed using a single [11,50] or two drugs [51–53]. For instance, Subhra et al. developed long-acting PLGA nanoparticles of tenofovir alfenamide and emtricitabine eliciting anti-HIV efficacy until 14 days [53]. While Zhiyi Lin developed abacavir nanoprodrug, which depicted antiretroviral effect till 30 days [54]. However, HIV treatment involves the administration of conventional antiretroviral (ARV) formulations by oral route along with injectable LA ARV nanoformulations, which may lead to drug-drug interaction and toxicity [17]. Amongst oral cART population, 28% lack adherence [55] due to high frequency of administration. Moreover, orally administered drugs elicit decreased bioavailability due to hepatic first pass metabolism and drug-drug interaction due to the presence of various transporters and metabolic enzymes in intestinal epithelium, which can be avoided by LA nanoformulations [56]. Therefore, those physicochemical properties of the drugs, which determine stability, bioavailability and efficacy of LA ARV nanoformulations become vital [57,58]. In case, physicochemical properties of the orally administered drugs are not suitable for LA nanoformulation, new drug synthesis for LA effect is required [56]. Generally, orally administered active pharmaceutical ingredients (APIs) must satisfy the Lipinski rule of five. The rule states that APIs which exhibit molecular weight, log P, hydrogen bond donors and acceptors as < 500 Da, < 5, 5 and 10 respectively, are considered good candidate for oral delivery [59–61]. The similar, rule could be extended to understand the properties of APIs suitable for LA nanoformulations. Further, other physicochemical properties including solubility and pK_a played a significant role in the design of LA ARV nanoformulations. Those drugs which exhibit low aqueous solubility (< 50 mg/ml), high log P (2-5), high potency with low therapeutic plasma drug concentration (< 1000 ng/ml), and low pK_a are considered suitable for LA effect [56]. Higher pK_a of the drug leads to ionization at physiological pH below 7.4, causing increased drug solubility and electrostatic interaction between drug and excipients. Therefore, esterification of drug to form prodrug with increased pKa leads to decreased dissolution of drug leading to longer half-life and increased potency [62]. For instance, cabotegravir was esterified to form myristoylated prodrug [11],emtricitabine converted to palmitoylated emtricitabine [63], lamivudine and abacavir to phosphoramidate pronucleotide [64] and rilpivirine to methyl tetradecanoate prodrug [50] to prepare LA nanoformulations. The pharmacokinetic of the drug depends upon the drug release from LA nanoformulation, solubility, molecular weight and log P. Therefore, for dual drug LA nanoformulation the pharmacokinetic of individual drug should be similar to avoid lack of effective plasma and site-specific concentration of either drug after certain time post administration [57,65]. Further, particle size of LA nanoformulations played a significant role in producing therapeutic effect for longer duration. For instance, rilpivirine nanosuspension (200 nm) stabilized by poloxamer 338 depicted higher drug loading and sustained plasma concentration in humans compared with 400 nm and 800 nm vitamin E TPGS stabilized rilpivirine nanosuspension when injected by IM or SC, which showed plasma concentration below 10 ng/ml after 3 or 6 months respectively. Further, the rilpivirine LA nanoformulation (200-600 mg dose) showed plasma concentration (73-95 ng/ml) above mean minimal concentration as obtained by daily once oral dosing. However, no difference was observed in plasma concentration after SC or IM route, ruling out the role of route of administration on LA potential of nanoformulations with different physicochemical properties in the same species [66]. Moreover, polarity of the drug also played a significant role in solubilization and absorption. It was observed that polar surface area (PSA) of 63°A elicited 90% oral bioavailability while, only 10% oral bioavailability was exhibited for PSA of 139°A [67].

The suitability of the drug for LA nanoformulations should rather consider the Biopharmaceutical Drug Disposition Classification System (BDDS) wherein, class I and II consist of high solubility/extensively metabolized and low solubility/extensively metabolized API respectively. In contrast, class III and IV include high solubility/poorly metabolized and low solubility/poorly metabolized API [68]. The BDDS classification for drugs was an extension to Biopharmaceutical Classification System (BCS) after observing the drug disposition mechanics in each class to predict drug absorption as well as disposition. The BDDS classification categorizes drugs into four groups wherein class I and II drugs lead to metabolic disposition in contrast to class III and IV which were eliminated by urine or bile. Drugs belonging to BDDS class II are the substrate for P-glycoprotein efflux, class III drugs are subjected to absorptive transporter effect while, class IV are susceptible for efflux and absorptive transporter [69]. Thus, BDDS classification determines the transporter, enzymatic substrate and drug-drug interaction in liver, intestine, kidney and brain. Generally, class II and IV drugs are suitable for lipid-based nanoformulations wherein transporter modifying carriers could be used. Moreover, both class II and IV drugs lead to significant reduction in dose with $> 70\%$ and $< 30\%$ metabolism, respectively [69]; making these candidates suitable for LA nanoformulation. Further, poorly metabolized drugs exhibit sustained drug release potential due to low clearance. Therefore, proper *in-vitro in-vivo* correlation needs to be established along with an estimation of site-specific concentration and toxicity profile of BDDS class IV drug, if incorporated into LA nanoformulation [70]. Effective delivery of long-acting nanoformulations requires lower dose volume for administration. Therefore, those drugs which exhibit short half-life and high dose serve as poor candidates for LA nanoformulation, probably due to the requirement of high injection volume for administration [17]. Moreover, the drug must be stable when exposed to varying enzymes and pH *in-vivo* [71].

2.2. Impact of route of administration on in vivo behaviour of long-acting nanoformulations

Both oral and parenteral routes have been explored for LA ARV nanoformulations based therapy. Kirtane et al. developed once weekly gastric resident dosage form administered orally consisting of a central core and five arms comprising different polymers and drug matrix of dolutegravir, rilpivirine, and cabotegravir individually in 4 different arms. The arms are composed of elastomeric polymer core, which can coil into capsule and recoil upon dissolution of capsule shell in the stomach. The design allowed to load different polymer and drug matrix in different arms with different release rate. The plasma drug concentration was comparable to C_{max} for dolutegravir and rilpivirine while, 2.5-fold less than C_{max} for cabotegravir until six days. While the plasma drug concentration fell below the detection limit within two days from the immediate release dosage form of each drug in pigs (n = 3). The dosage forms showed the advantage of no-drug interaction and administration of drug-loaded nanoparticle matrix in individual arm. However, the polymeric device, due to its non-biodegradable nature, needs to be retracted from gastrointestinal tract (GIT) after seven days [72]. Further, gastro-retention of the dosage form was a function of gastric emptying time and rate along with the type of food which may differ amongst every individual. Also, ARV with only lower doses could be incorporated into the individual arm due to the limited size of the dosage form. Additionally, the formulation may fail to sustain constant intracellular drug levels if the formulation was not administered on the same day and same time after a week once levels of the drug decreased at day 7.

Drug-loaded nanoformulations when administered parenterally via subcutaneous or intramuscular route showed therapeutic effect for several months. The long-acting effect of these nanoformulations could be due to the formation of depot at the site of administration to enable sustain drug release for extended period of time. Sequestration of nanoparticles from depot into lymphocytes [12] or macrophages [50,73] to form secondary depot for long term slow release of the drug is another reason of long-acting effect. Intravenous infusion has also been utilized for long-acting anti-HIV effects. For instance, Vedolizumab is long-acting humanized immunoglobulin [2-R-monoclonal antibody which binds to α4β7 integrin and inhibit the virus entering the $CD4^+$ T cells administered as IV infusion for 30 min depicted serum half-life of 25 days [74]. It has been reported that both subcutaneous and intramuscular route showed sustained drug release of nanodrugs independent of particle size [75]. However, the absorption via intramuscular route is fast as compared to subcutaneous route, making it suitable for administration of oil based LA nanoformulations. For instance, when pharmacokinetic after IM and SC administration of long acting rilpivirine nanosuspension was compared, it was observed that SC route elicited sustained plasma concentration for 6 months, than IM upto 3 months in beagle dogs. Further, The C_{max} was significantly higher (4.5-folds) with decreased T_{max} (6-folds) for 5 mg/kg IM rilpivirine nanosuspension compared with SC rilpivirine nanosuspension (200 nm). IM administration of rilpivirine nanosuspension led to rapid onset of action because of higher draining effect due to the presence of blood capillaries when compared with SC [76]. While, administration of rilpivirine nanosuspension in humans by SC and IM route led to similar C_{max}, the T_{max} was 1.83 folds lower at 100 mg IM dose. Therefore, although both the routes led to similar plasma concentration, the duration of action was prolonged by the SC route. The tissue to plasma ratio of rilpivirine administered via SC was 1.25-folds and 1.47-folds higher in the cervix and vagina, respectively, when compared to IM route [58]. On the contrary, clinical trial of cabotegravir long-acting nanosuspension in 72 human volunteers demonstrated comparable C_{max} (0.166-0.644 μg/ml) and median half-life of 69 days when administered via both SC and IM route [77]. Therefore, along with the route of administration, other factors including the difference in muscle mass, gender, fat distribution, injection technique, and physical activity might also be the cause of variation in the rate of absorption and maintenance of desired plasma concentration. To conclude, both SC and IM route of administration may provide sustained drug delivery for longer duration and could, therefore, be preferred for LA nanoformulation delivery. However, an enhanced duration of action with increased tissue/plasma ratio could be obtained by administration via subcutaneous route.

2.3. Role of the circulatory and lymphatic system in enhancement of bioavailability of long-acting antiretroviral

Both circulatory and lymphatic systems play a significant role in targeted delivery of ARV drugs. When high pressure is built in tissues, the blind-ended lymphatic capillaries, which consist of endothelial cells, unidirectional valves open and drain the interstitial fluid into the lymph vessels to thoracic ducts which then accumulate into collecting valves and draining into the left subclavian vein. Hydrostatic pressure head (generally between 0.2-0.8 cmH_2O) is the primary driving force for draining the interstitial fluid into lymphatic vessels [78].

Furthermore, a suction force is also generated during the resting phase of the vessels, which further contributes to the accumulation of interstitial fluid into the lymphatic vessels [78]. In contrast to tight junctions present in the endothelial cells of the blood capillaries, the lymphatic valves are composed of fenestrated endothelial cells, forming a pore of 2 μm. Therefore, large molecules can rapidly enter into the lymphatic system [79]. The lymphatic muscles aid in slow phasic contraction and relaxation of vessels as compared to blood capillaries (10/min) [80], which could enable longer retention of nanoparticles when absorbed and distributed via the lymphatic system, thereby enhancing the bioavailability of the drug. HIV replication occurs predominately in lymphoid organs and lymph nodes throughout the body. It was reported that after treatment with cART in SIV-rhesus macaque for one year, the plasma viral load was suppressed. However, the viral RNA was observed in different organs in the order of lymphatic tissues > lungs and intestine > other tissues [81]. The lymph nodes are a major site of viral hub for replication and retention in germinal cells and CD4+ T cells. Therefore, viral rebound may occur due to viral residues in the lymph node [82]. Increased absorption in the lymphatic system through lymphatic plexus in subcutaneous and skeletal muscles, therefore, could enhance the effectiveness of LA ARV nanoformulations. Particle size of nanocarriers has also been reported to play a crucial role in the distribution of LA nanoformulations via the lymphatic system. Upon SC/IM administration, nanoparticles of larger size could form a depot. Depending upon the physicochemical properties, drugs will be absorbed by either the lymphatic or blood circulatory system. For instance, < 100 nm particles could be absorbed by the lymphatic system, thereby enhancing circulation time and bioavailability [83]. HIV infected macrophages are known as a site for proviral HIV persistence. Macrophage at injection site engulfed LA nanoformulation passed through the lymphatic system slowly into systemic circulation which resulted in slow release of drugs from macrophage LA nanoformulation depot [84]. Nanoparticles with a hydrophobic surface and larger particle size (> 200 nm) tend to be phagocytosed upon intravenous administration [85]. This strategy can be well explored for long-acting slow release of drugs from macrophages. For instance, higher accumulation of zidovudine myristate loaded liposomes were observed in reticuloendothelial organs and brain after IV administration due to phagocytosis of liposomes [86]. Dou et al. demonstrated the release of indinavir from the macrophage-based system for 14 long days and suppressed viral load significantly in the brain after intravenous administration in mice [87]. Nucleoside reverse transcriptase inhibitors (NRTI)and protease inhibitors (PI) have the inherent potential to target endosomes of macrophages and elicit antiretroviral effect [84]. For instance, Atazanavir nanoART led to the highest accumulation in macrophage compared to granulocytes and differentiating cells, further higher concentration of drug was obtained in spleen > liver > lymph

node when administered via intraperitoneal and intramuscular route [88]. Therefore, LA nanoprodrug or LA nanocrystal could form effective depot in macrophages which ultimately enter into the lymphatic organs from blood circulation and further enhance half-life and bioavailability of antiretroviral drugs.

3. Long-acting antiretroviral nanoformulations

Various nanoformulations including nanocrystals [89], nano-prodrug [11,50], solid drug nanoparticles [90], lipid [65,91–93] and polymeric nanoparticles [94,95] and nanosuspension [96,97] have been explored for LA ARV effect. The method of preparation and long acting slow effective release potential of LA ARV nanoformulations have been presented in Fig. 1. Currently, few drug candidates have been scaled up to clinical trials. In contrast, a few LA ARV nanoformulations have shown promising results during preclinical studies, which can be progressed towards clinical development. The preceding section deals with LA ARV nanoformulations which have shown promising results in preclinical and clinical studies

3.1. Long-acting antiretroviral nanoformulations under clinical trials

ARV nanocrystals have recently reached late stage clinical trial. It is widely utilized technique to improve the solubility, bioavailability, and drug loading of poorly soluble drugs. Moreover, nanocrystals, when stabilized with a small amount of surfactants to form nanosuspension, offer advantages associated with nanoformulation and overcome the challenges related to regulatory, toxicological, and scalability of the nanoformulations [75]. These nanocrystals have been reported to form depot at the injection site after SC or IM administration. The drug is released slowly from the depot, probably due to hydrophobic nature and subsequently drained into thoracic lymphatic vessels, due to the particle size suitable for physical filtration into the lymphatic sinuses. The drug, from the lymphatic system, could slowly release into the systemic circulation, leading to long-acting antiretroviral effect [12]. While, upon intravenous administration, nanocrystals phagocytosed by macrophages, which acted as a drug reservoir, resulted in slow drug release in systemic circulation [98]. The creation of more hydrophobic prodrugs and further converting it into nanocrystals has also been attempted to develop LA ARV nanoformulations [63]. Various LA nanocrystals formulations of antipsychotic drugs, including Risperdal Consta [99] and Invega sustenna [100] incorporating Risperidone and paliperidone by Janssen and Zyprexa® Relprevv™ incorporating Olazapine by Eli Lilly are currently present in the market [101]. Based on these strong leads, LA nanocrystal technology was recently exploited for antiretroviral drugs. For instance, nanosuspension of single drug rilpivirine and cabotegravir, stabilized with poloxamer, polysorbate and/or polyethylene glycol are now under Phase III clinical trial [102,103]. Rilpivirine is a diarylpyrimidine containing non-nucleoside reverse transcriptase inhibitor (NNRTI), which is sparingly soluble in both aqueous and oily solvents and active against HIV-1 strain. It is the only low dose antiretroviral NNRTI (25 mg of daily dose), making it a suitable candidate for LA nanoformulations. Therefore, rilpivirine nanosuspension (200 nm) was developed by wet bead milling using poloxamer 338 as a stabilizer [97]. Preclinical studies were carried out in Sprague Dawley rats (250-350 g) and male beagle dogs (8-16 Kg) after administration of 5 mg/kg and 20 mg/kg via either SC or IM route leading to detectable drug level till 42 days. The nanosuspension showed dose-dependent kinetics in both rats and dogs with absolute bioavailability of 70-80% and 80-102%, respectively. The drug concentration in different organs was found to be in the order of lymph node > thymus > brain = spleen > plasma. [66]. Successful tolerability and pharmacokinetic profile, led rilpivirine nanosuspension as potential preclinical candidate transferred into clinical trial (Table 2). Another integrase inhibitor (Cabotegravir) was also found to be suitable for the creation of long-acting nanoformulation due to promising anti-viral potency, low frequency of administration, longer half-life, stability as well as low adverse effects [96,104]. Therefore, cabotegravir long-acting nanosuspension (200 nm) was prepared by wet bead milling using polysorbate 20 and polyethylene glycol 3350 as surfactant. Preclinical studies of [^{14}C]-Cabotegravir in male rats, mice, and monkeys revealed that the 50% radioactivity in all the tissues 28-days post-dosing. Blood showed higher radioactivity at all the time-points compared with other tissues from day 1 till 28 days post IM or SC dosing. Spleen contained the highest radioactivity (18%) amongst all other HIV hub organs [104]. Further, the presence of macrophages at the site of administration could cause slow cabotegravir release from macrophages, causing an increased terminal half-life of 39-41 h [105,106]. Further, LA cabotegravir (50 mg/kg) also showed potential as PrEP in intravenously 17AIDS$_{50}$SIVmac251 challenged macaques with 88% protection [107]. Further, on cervical exposure of SHIV162P3 in female macaque depicted no viral infection with plasma concentration of cabotegravir above IC$_{90}$ up to 8 weeks [108]. Due to successful plasma pharmacokinetic profile, biodistribution, and PrEP ability of cabotegravir long-acting nanosuspension, it was further led to clinical trials (Table 2). Furthermore, sustained HIV suppression can be achieved with cART emerging the need of combination therapy involving other drugs administered orally compared with single LA nanoformulation. Therefore, ViiV healthcare proposed increased ARV potency of cabotegravir and rilpivirine over single drug therapy after successful ATLAS and FLAIR clinical trial (Table 2) [109] with no drug interaction and pharmacokinetic interference of other drugs [96]. The outcome of successful ATLAS and FLAIR trial led to Health Canada approval of Cabenuva™ by Jannsen Pharmaceutica (Beerse, Belgium) on 20th March, 2020 for once monthly administration of cabotegravir and rilpivirine long-acting nanosuspension recommended for HIV-1 infected adults with suppressed and stable viral load [110]. Therefore, nanocrystals have served crucial role in development of LA formulations for enhanced efficacy and safety replacing the three-drug therapy evolved since 1996 [111] with two-drug daily administration.

3.2. Long-acting antiretroviral nanoformulations from in vitro hit to preclinical studies

3.2.1. Long-acting solid drug nanoparticles

SDN are drug/prodrug nanocrystals stabilized with surfactant and exhibit high drug loading (> 25% w/w) with extended-drug release profile [131]. Fast regulatory approval (especially, if the drug is FDA approved), long-term stability, improved bioavailability, flexible pharmacokinetic profile, and ability of cellular/tissue targeting are certain advantages of LA SDN [131–133]. Moreover, due to enhanced hydrophobicity and reduced particle size, it revealed a higher intracellular accumulation compared to the free drug [134]. After the successful clinical trials of low dose cabotegravir and rilpivirine nanocrystal nanosuspension, SDN have been explored as a long-acting injectable for sparingly soluble antiretroviral drugs of high doses (150-600 mg BID). For instance, Owen et. al. developed long-acting maraviroc SDN (750 nm) using polyvinyl alcohol (PVA) and 1,4-bis-(2-ethylhexoxy)-1,4-dioxybutane-2-sulfonate (AOT) with 70%w/w drug loading. *In vivo* intramuscular administration in adult male Wistar rats (10 mg/kg) revealed detectable plasma concentration of maraviroc SDN up to 240 h in comparison to free maraviroc solution (5% DMSO) which was detected until only 72 h. The AUC$_{0-\infty}$ and terminal half-life was 3.45 and 2.64-folds higher, respectively with 2-folds decrease in T$_{max}$ for Maraviroc SDN compared with free Maraviroc 1-week post-dosing. However, SDN needs to be further evaluated to extrapolate the data for other species, to depict its clinical benefits [90,135].

3.2.2. Long-acting nanocrystals

After the successful advent of cabotegravir and rilpivirine nanocrystal based nanosuspension into phase 3 clinical trial and its subsequent new drug application appeal to FDA by ViiV Healthcare [136],

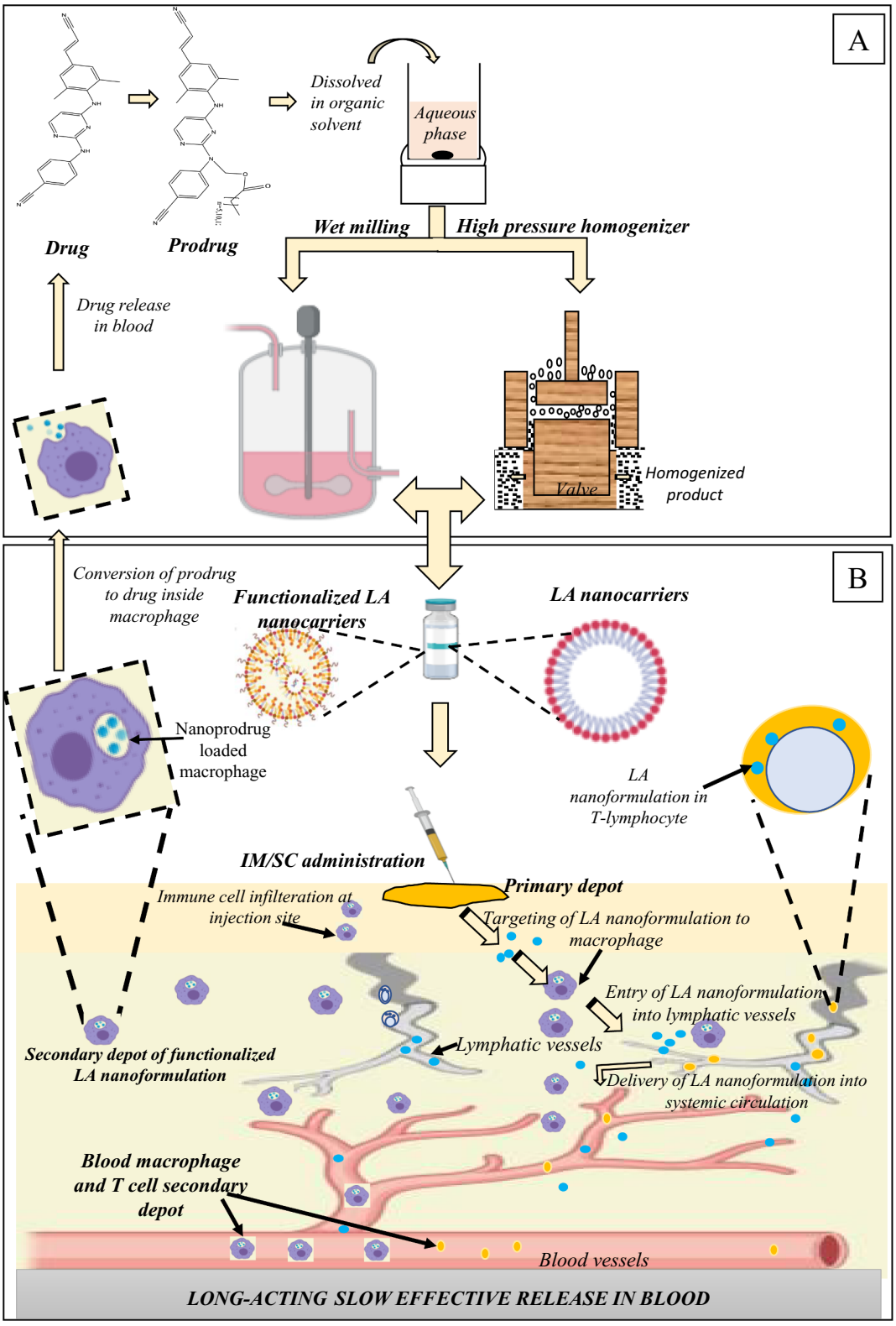

Fig. 1. Schematic presentation of (A) Method of preparation of long-acting nanoformulations. (B) Mechanism of lymphatic and immune cell targeting of long-acting nanoformulations after subcutaneous or intramuscular administration.

nanocrystal technology has been enticing for the scientific community for LA nanoformulation development. For instance, preclinical studies of LA nanocrystals (nanoART) of atazanavir (nanoATV) and ritonavir (nanoRTV) depicted LA effect due to tissue macrophage depot when administered in mice and monkeys by subcutaneous and intramuscular route, respectively. Acute single dosing of NanoATV revealed 13- and 41-fold higher concentrations in plasma and tissue, respectively, as compared with free ATV. Moreover, multiple dosing (at day 0, 3 and 7) of nanoATV revealed 270-folds higher serum and tissue concentration of ATV compared with free ATV for up to 8 weeks. Both nanoATV and

Table 2
Summary of clinical trials of Rilpivirine and Cabotegravir long-acting nanosuspension

Drug	Organization	Clinical trial	Study duration	Study design	Study remarks	References
				PrEP		
Rilpivirine	PATH (Seattle)	Phase 2a (HPTN 076)	10/2014-04/2015	✓ 136-HIV negative women aged 18-45 years were administered LA rilpivirine nanosuspension for PrEP in double blind, 2-arm study	✓ No specific side effects ✓ 80% of the population preferred LA injectable against implants ✓ Better tolerability and acceptability was observed compared to oral daily dosing	[112,113]
Cabotegravir	ViiV Healthcare (United Kingdom)	Phase 1	04/2018-04/2020	✓ 48 low risk healthy Chinese men between 18-65 years of age ✓ Once daily oral administration of Cabotegravir (30 mg) for 4 weeks followed by 4-weekly administration of cabotegravir LA (600 mg) at week 5,9,17,25 and 33.	–	[114]
	ViiV Healthcare (United Kingdom)	Phase 2a (ÉCLAIR)	03/2014-05/2015	✓ 127 HIV healthy males (18-65 years) to study the safety, tolerability and acceptability of cabotegravir LA nanosuspension	✓ Only 2% acquired HIV infection one in placebo group and other in cabotegravir group where protein binding was below IC_{90} value ✓ Grade 2 adverse events were higher ✓ Apparent terminal half-life was 40 days ✓ Pharmacokinetic study revealed administration of 800 mg every 12 weeks was suboptimal ✓ LA injectable cabotegravir can be used as alternative to daily oral cabotegravir for PrEP	[115]
	National institute of allergy and infectious disease (NIAD) (United States)	Phase 2a (HPTN-077)	02/2015-05/2016	✓ 443 healthy individuals aged 18-65 years participated in randomized double-blind placebo control trial to assess safety, pharmacokinetic and tolerability against oral once daily cabotegravir tablet ✓ Administration of 3 cabotegravir LA (800 mg) injections every 12 weeks in cohort 1 while, 5 injections of cabotegravir LA (600 mg) wherein 2 injections with gap of 4 weeks and remaining 3 injections in the duration of 8 weeks in cohort 2	✓ 11% participants out of the oral group discontinued the oral study product ✓ Adverse events were only grade 1 and 2 type, however, did not lead to discontinuation of injectable cabotegravir LA ✓ 95% population in cohort 2 had plasma concentration above $IC_{90,}$ out of which 80% population had plasma concentration 4-times higher than IC_{90} of cabotegravi	[77]
	ViiV Healthcare (United Kingdom), Gilead Sciences (United States)	Phase 2b/3 (HPTN-083)	12/2016-03/2022	✓ 5000 participants of healthy cisgender men and transgender women who have sex with men to evaluate safety and tolerability of cabotegravir long acting nanoformulation after IM administration of 600 mg against daily oral dosing Tenofovir disproxil fumarate/emtricitabine(TDF/FTC) (300/200 mg)(FDC)	–	[116]
				HIV-1 treatment		
Rilpivirine	Jannsen research and development, LLC (Ireland)	Phase 1	01/2010-07/2011	✓ Initially, 6 (300 mg/ml) and 5 (600 mg/ml) healthy human volunteers of either sex ✓ In second part, participants were administered with 3 IM injections of 1200, 600 and 600 mg every 4-week for 3 months in double-blind placebo control group	✓ Both single dose and multiple doses of rilpivirine led to favourable local/systemic tolerability ✓ The plasma concentration was comparable after loading dose (1200 mg) and maintenance doses (600 mg) with 79 ng/ml concentration after 30 days of last dose administration, suggesting clinically significant plasma concentration could be achieved	[117]
	Jannsen research and development, LLC (Ireland)	Phase 1	11/2012-01/2016	✓ 24 women and 12-males enrolled for open label study out of which 12 women and 6 men received 1200 mg/600 or 1200 mg loading/ single maintenance dose via IM route	✓ 200 adverse events of grade 1-2 ✓ Tissue/plasma ratio was 2-folds higher in rectal compared to cervix/vagina ✓ Rectal biopsy caused viral suppression when exposed *ex vivo*. No viral suppression was observed when cervical and vaginal tissues were exposed.	[118]

(*continued on next page*)

Table 2 (*continued*)

Drug	Organization	Clinical trial	Study duration	Study design	Study remarks	References
				PrEP		
Cabotegravir	ViiV Healthcare (United Kingdom)	Phase 1	02/2017-07/2019	✓ 8 HIV negative males and females in each cohort study. ✓ 9 cohorts, open label parallel study at 100-800 mg IM and 100-400 mg SC. The study was conducted after single dosing cabotegravir LA administration (200 mg/ml nanosuspension) ✓ Open label parallel group multicentre study, involving 8 participants with severe renal impairment	✓ In case of 800 mg dose plasma concentration was above IC_{90} for 16 weeks ✓ Mild adverse events observed ✓ Safe for once monthly administration ✓ Safe for participants with renal impairment without dose adjustment	[119–121]
Cabotegravir + VRC07-523LS	NIAD (United States)	Phase 3	12/2019-01/2023	✓ 74 HIV-1 infected adults with suppressed plasma viremia to assess safety, tolerability, pharmacokinetic and antiviral activity of LA cabotegravir and monoclonal antibody(VRC07-523LS) intravenous infusion with discontinued ART except for NRTI	–	[122]
Cabotegravir + Rilpivirine	ViiV healthcare (United Kingdom)	Phase 2b	08/2018-01/2021	✓ Open label, multicentre, rollover study including 98 HIV-1 positive participants wherein one group will receive LA (cabotegravir + rilpivirine) nanosuspension bimonthly or oral dolutegravir and rilpivirne	–	[123]
	ViiV Healthcare (United Kingdom)	Phase 2b (LATTE-2)	04/2014-11/2016	✓ 309 participants were involved in open label study HIV-1 infected treatment naïve adults (> 18 years) ✓ 20 weeks oral cabotegravir (30 mg) plus abacavir (600 mg)-lamivudine (300 mg) followed by LA IM cabotegravir (400 mg) + Rilpivirne (600 mg) 4-weekly or cabotegravir (600 mg) + rilpivirine (900 mg) 8-weekly	✓ After 32 weeks 94% and 95% viral suppression was maintained in 4-weekly and 8-weekly group respectively. ✓ After 96-weeks viral suppression was maintained in 84% and 87% 4-weekly and 8-weekly group respectively. ✓ Two-drug LA combination was as effective as oral regimen and led to viral suppression upto 96 weeks	[124]
	ViiV Healthcare (United Kingdom)	Phase 3 (ATLAS)	10/2016-05/2018	✓ 618 HIV-1 infected adults with randomized, multicentre parallel, open label trial ✓ Patients with FDC of abacavir, lamivudine and dolutegravir	✓ Once monthly LA regimen of cabotegravir + rilpirivirne was comparable to 3-drug oral ART at 48 weeks	[125,126]
	ViiV Healthcare (United Kingdom)	Phase 3 (FLAIR)	10/2016-08/2018	✓ 631 HIV-1 infected adults were selected to determine safety, efficacy and tolerability of LA cabotegravir (400mg) + rilpivirne (600mg) who were earlier of abacavir/dultegravir/lamvudine single tablet regimen in 48 weeks study	✓ 2.1% and 2.5% in LA group and oral regimen group had viral RNA ≥ 50 c/ml at 48th week and 1.4% had confirmed virological failure in LA group ✓ 99% were satisfied with cabotegravir + rilpivirine LA therapy compared with oral regimen	[127,128]
	NIAD (United States)	Phase 1and 2	03/2019-05/2022	✓ 155 HIV- 1 infected children and adolescent were included in the study to determine the dose of oral and IM LA cabotegravir and Rilpivirne which will be administered in addition to their general cART therapy in cohort 1 ✓ After cohort 1 full data analysis is done further studies will be carried out without cART regimen but, with oral Cabotegravir and rilpivirne followed by IM cabotegravir plus rilpivirine LA	–	[129]
	NIAD (United States)	Phase 3	03/2019-09/2022	✓ 350 HIV-1 infected participants with sub-optimal adherence history to check the viral suppression via either cabotegravir+ rilpivirin LA or with standard oral ART	–	[130]

Study duration has been represented as mm/yyyy

nanoRTV were accumulated in the non-lysosomal compartment of tissue macrophages [89]. In order to achieve targeted delivery with enhanced macrophage uptake of LA nanoformulation, surface conjugation [51] have been explored. Tissue-specific macrophages, including liver, spleen, lymph node, gut-associated lymphoid organ, and brain express folic acid receptor (FA-R) onto the cell surface. Targeting of antiretroviral drugs to cell-based and tissue-based FA-R expressing macrophages could enhance LA nanoformulation efficacy. Therefore, nanoART stabilized with folic acid-conjugated poloxamer 407 incorporating atazanavir boosted with ritonavir (FA-nanoATV/r) were developed. The plasma concentration of RTV did not differ between FA-nanoATV/r and nanoATV/r. While the plasma concentration was increased by 2.3-folds for ATV when FA-ATV/r was administered as compared to non-functionalized nanoATV on day 14 post-IM administration. Also, 5-folds increase in bioavailability with a 5-fold reduction in dose of FA-nanoATV/r was obtained [137]. Secondary macrophage depot, along with injection site depot, was confirmed by a biphasic plasma profile of FA-nanoATV/r. The biodistribution of FA-nanoATV/r in HIV reservoir sites, including spleen, liver, lymph node, kidney, lungs and plasma were significantly higher compared with nanoATV/r 14 days post-administration. The ratio of CD4/CD8 count was restored by 17% in the case of FA-nanoATV/r (50 mg/kg) treatment group as against only 3% in PBS treated group in infected mice. FA-nanoATV/r led to a significant reduction in P24 level in liver and spleen and HIV-1_{gag} RNA levels in the spleen compared with nanoATV/r and untreated group. Therefore, macrophage targeted FA-nanoATV depicted potential of LA nanoformulations as once biweekly administration with a 5-fold reduced dose [51].

3.2.3. Long-acting nano-prodrug

Monthly/bimonthly LA nanoformulation administration exhibits major challenge associated with relatively high dose and volume of adminsitration. Prodrugs could be viable alternatives to further enhance the potency by slow conversion to parent molecule leading to slow effective plasma concentration. For instance, cabotegravir LA nanocrystal nanosuspension requires to divide into two injections (2 ml each) to administer 800 mg dose. Further, in ÉCLAIR trial 2/3rd population had plasma concentration below 4*IC_{90} of cabotegravir, which urges for increased frequency of administration by IM route. Further, the IM cabotegravir depot was rapidly absorbed from the injection site [105]. These observations resulted in the creation of a prodrug of cabotegravir with more hydrophobicity than the parent drug, to prevent fast release, achieving sustained plasma level and decreased dosing regimen. For instance, fourteen carbon myristoylated prodrug of cabotegravir (MCAB) showed 1.24-folds lesser IC_{50} value than cabotegravir against HIV-1_{ADA} in MDM. Nanoformulations of myristoylated cabotegravir (NMCAB) and cabotegravir (NCAB) were prepared using poloxamer 407 to form rod-shaped particles. These rod-shaped particles could be phagocytosed by macrophage and were stable up to 90 days. Cell uptake studies revealed that NMCAB were phagocytosed by macrophages 60- to 88-folds higher compared with Cabotegravir long-acting parenteral (CAB LAP) formulation and NCAB respectively. NMCAB crystals were observed inside macrophages depicting the conversion of prodrug MCAB to CAB (Fig. 2A). Treatment with NCAB and CAB LAP showed an increase in RT level by 70 and 84% on day 15 while, NMCAB treatment caused sustained RT inhibition in HIV-1_{ADA} infected MDM cells (Fig. 2B). IM administration in BALB/cJ mice elucidated sustained plasma level (above 4*IC_{90}) up to day 56 for NMCAB (45 mg/kg) while; it fell below 4*IC_{90} on day 35 in case of CAB LAP. 4-fold higher plasma half-life and volume of distribution while, a 2-fold increase in mean residence time (MRT) was observed upon NMCAB treatment compared to CAB LAP. Lung, Liver, kidney, gut, and spleen depicted CAB concentration above PA-IC_{90} in NMCAB group, unlike CAB-LAP treated group. Further, in rhesus macaque, the half-life was 2-4 folds higher for NMCAB (45 mg/kg) compared with CAB-LAP (45 mg/kg). Also, secondary tissue depot and immune cell depot of NMCAB were confirmed by higher MCAB concentration in liver, lung, spleen, and lymph node as against blood after 24 h as well as in infiltered immune cells at the injection site (Fig. 2C-D). The reduced viral DNA, RNA, and p-24 expressions in tissues were correlated with > 5-fold increase in cabotegravir amount in those tissues upon administration with NMCAB. Thus, NMCAB depicted the potential to increase dosing interval with reduced dosage and dosing volume in preclinical findings [11]. Similarly, poloxamer 338 or 407 stabilized N-acylalkoxy rilpivirine (RPV) prodrug nanoformulation (NM3RPV) was synthesized to achieve long-acting slow effective release (LASER) up to 25 weeks. The stability of NM3RPV was comaparable with nanoformulated RPV (NRPV) at 4°C and 37°C over 100 days. NM3RPV was retained into MDM cells for 30 days. While, RPV level, in case of rilpivirine nanocrystal suspension (NRPV), reduced below the limit of quantification by day 20. Further, > 90% viral suppression in HIV-1_{ADA} infected MDM cells up to 30 days when treated with NM3RPV (10 μM and 30 μM) was achieved as against only 67% protection up to day 10 with relapse occurring at day 20 upon NRPV treatment. The plasma concentration of RPV was maintained above PA-IC_{90} value (12 ng/ml) up to 25 weeks as against 16-weeks after IM administration in BALB/cJ mice treated with NM3RPV and NRPV respectively. Further, 13- and 26-folds increase in $t_{1/2,}$ and MRT was observed when treated with NM3RPV. Further, RPV was detected in all the tissues (spleen, lymph node, liver, gut, kidney) after 46 weeks in NM3RPV treated group with the highest concentration in lymph node (145 ng/g) while no RPV was detected in NRPV group. In rhesus macaque, the plasma concentration of NM3RPV was 2- to 16-folds higher compared to RPV up to 44 weeks. Further, detectable levels of RPV and NM3RPV was found in the lymph node, rectal and adipose tissue biopsies at 204 days (Fig. 2E) [50]. Prodrug nanoformulations have also been created to obtain LA slow release for the highly hydrophilic drug by enhancing their hydrophobicity. For instance, palmitoylated emtricitabine (FTC) prodrug nanoformulation (NMFTC) was prepared using poloxamer 407 as a stabilizer by high-pressure homogenization. The prodrug revealed a decrease in aqueous solubility of FTC by 1200-folds, and was found to be stable for ten weeks. Further, NMFTC was more effective in suppressing 100% viral load up to ten days when challenged with HIV-1_{ADA} after 8 h. In contrast, only 24 h viral suppression was observed in the case of FTC nanoformulation (NFTC) treated group in HIV-1 $_{ADA}$ infected cells. Plasma concentration of FTC was only 5-fold lower than IC_{50} upon IM administration of NMFTC compared to 8-fold lower than IC_{90} with NFTC by day 14 post IM treatment. Biodistribution studies revealed a higher concentration of FTC in the liver, spleen, and lymph node in the NMFTC group up to day 7 with a detectable concentration in the lymph node on day 14 only in NMFTC treated mice. Further, a significantly higher concentration of FTC-triphosphate (a metabolite of NMFTC) was observed in PBMC and lymphoid cells of spleen and lymph node. Thus, NMFTC effectively enhanced drug delivery to viral reservoirs with reduced dosing frequency compared to available once-daily oral regimen encompassing the inability to target HIV prone cells [63]. Many other antiretrovirals, including darunavir [138], lamivudine [64,139], abacavir [54], and dolutegravir [140] have been recently explored for conversion into prodrug nanoformulation with efficient LA slow-release potential in preclinical studies. Pharmacokinetic characteristics of these LA nanoformulations are presented in table 3.

3.2.4. Long-acting polymeric nanocarriers

Polymeric nanocarriers have been widely utilized as long-acting nanoformulations due to the depot formation when administered via subcutaneous or intramuscular route. Polymeric LA nanoformulations necessitates the use of biodegradable and biocompatible polymers for drug delivery to avoid removal after the exhaustion of drugs. The hydrophobic nature of the polymers is another essential property to enable drug release over an extended period [141]. Further, hydrophobicity of the polymer could enable enhanced absorption of nanoparticles through lipophilic vessels [142]. Moreover, polymeric

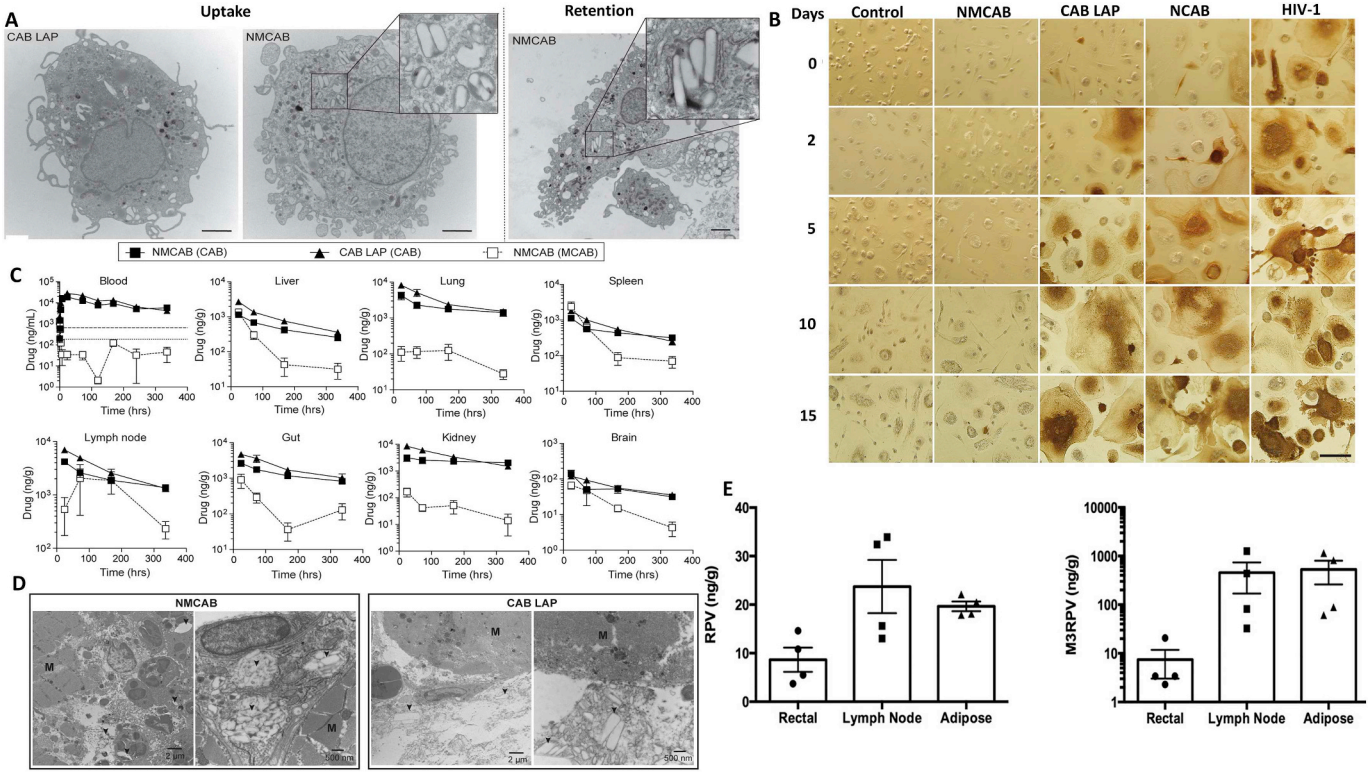

Fig. 2. *In vitro* studies (A) TEM image showing uptake and retention of rod shaped crystals post 8 h treatment with NMCAB (equivalent to 100 μM CAB) in MDM cells in contrast to CAB LAP treatment showing absence of crystal. (B) Antiviral activity of NMCAB, CAB LAP and NCAB upto 15 days against HIV-1_{ADA} in MDM cells in comparison with uninfected cells and untreated cells with HIV-1 p24 indicated with brown colour. *In vivo* studies (C) Blood and tissue concentration of NMCAB and CAB upto 14 days in Balb/cJ mice when administered with NMCAB and CAB LAP equivalent to 45 mg/kg CAB. (D) TEM image of cross section of muscle; imtramuscularly administered with NMCAB and CAB LAP. M depicts muscle fibre and NMCAB and CAB crystals are indicated by arrows [11]. (E) Tissue concentration of RPV and M3RPV determined after biopsy on day 204 after IM administration in macaques [50].

nanocarriers could encapsulate both hydrophilic [143] and hydrophobic drugs [52,94,144] for long-acting slow-release, by diffusion or dissolution of the drug/s from the polymeric nanocarriers [141]. Recently, efforts were directed to develop polymeric nanocarrier incorporating elvitegravir (EVG), tenofovir alafenamide (TAF) and emtricitabine (FTC) for LA effect to obtain the drug concentration similar to the daily plasma profile of Genvoya*, a marketed product available for HIV treatment. PLGA (lactide: glycolide ratio-75:25) was used to retard the release of hydrophobic (EVG and TAF) and hydrophilic (FTC) drugs for a longer duration. The LA nanoparticles (EVG + TAF + FTC NP) were effective for biweekly SC administration compared to the once-daily pill of Genvoya*, and the plasma viral load was suppressed over 22 weeks. Infra-red dye loaded PLGA nanoparticle revealed accumulation of nanocarriers in HIV infection site (female reproductive organ and colon), viral reservoir site (brain and spleen), and infection spread site (subclavicular, axillary and inguinal lymph node) at day 14 post SC administration. Moreover, the potential of nanoparticles for slow effective release was evident by high fluorescence at the injection site and draining organs including liver and kidney even after 14 days. Moreover, EVG + TAF + FTC NP showed 4-fold decrease in plasma viral load up to 22 weeks with maintenance of plasma CD4 level (> 80%) until 15 weeks. Viral rebound occurred by 24th week (4 weeks post EVG + TAF + FTC NP SC administration), suggesting need for biweekly administration of EVG + TAF + FTC NP. EVG + TAF + FTCNP was the the first proof of concept for LA cARV delivery. [95]. Three drug cARV have recently been replaced by two drug combination for pre-exposure (PrEP) prophylaxis. For instance, long-acting polymeric nanoparticles encapsulating TAF + FTC [53] and TAF + EVG [145] were designed to overcome the daily pill burden associated with Truvada® (TAF + FTC) [146]. TAF + FTC PLGA nanoparticles showed higher cell viability (88%) compared to TAF + FTC solution (60%) in TZM b1 cells. The plasma $t_{1/2}$, AUC_{all}, and vaginal tissue $t_{1/2}$ for TAF and FTC were found to increase by 2.2- and 28.33-folds, 4.2- and 19.5-folds and 6.5- and 9.3-folds respectively for TAF + FTC NP compared with TAF + FTC free solution upon SC administration in CD4 NSG mice. The required vaginal tissue concentration of TAF 14 days post TAF + FTC NP SC administration was 1.6-folds higher than required TAF vaginal concentration (6.8 ng/g). Interestingly, FTC tend to accumulate in the vagina while both TAF and FTC tend to accumulate in colon upon SC administration. Further, TAF + FTC NP (200 mg/kg) depicted 88% (day 4) and 60% (day 7 and 14) protection in Hu CD34 NSG mice when challenged with vaginal HIV-1 strain depicting its long-acting potential with enhanced tissue penetration ability [53]. The synergistic potential of EVG along with TAF was explored by developing long-acting TAF + EVG PLGA nanoparticles (TAF + EVG NP) for PrEP [52]. Upon SC administration in CD34$^+$ humanized nice, TAF + EVG NP depicted 8-folds and 5-folds increase in plasma $t_{1/2}$ for TAF and EVG, respectively; compared with their free drug solution. Further, drug concentration in vaginal and colon tissues at day 10 was greater or equivalent to that TAF and EVG concentration, which was obtained at 72 h upon SC administration of TAF + EVG solution. Long-acting PrEP potential of TAF + EVG NP was evident with the increased vaginal AUC by 2.7-3.9 times [145] for both drugs and 100% and 60% protection on day 4 and day 14 post-SC administration in vaginally challenged Hu BLT mice [52].

3.2.5. *Long-acting lipid nanoparticles*

In the case of LA nanoformulations under the late stage of clinical trials, administration of high dose antiretroviral drugs as a single injection is a significant challenge, which requires dividing large injection volume into multiple small volumes to administer the entire dose [115]. Incorporation of poorly soluble drugs in lipid-based nanocarriers (LNP) could be a promising strategy to overcome the above limitation due to

Table 3
Table 3 Summary of pre-clinical pharmacokinetic and efficacy studies for long-acting antiretroviral nanoformulation [161, 162].

Drug	Nanocarrier	Route of administration	Pre-clinical pharmacokinetic parameter and efficacy	Animal model for *In vivo* efficacy	Ref
Solid drug nanocarriers					
Maraviroc	PVA stabilized SDN (750nm;<0.5;70%) First order kinetics with 22.7% and 10% slower release compared to free Maraviroc in transport buffer and simulated intestinal fluid (SIF)	IM	***Species: Wistar rats*** Maraviroc SDN: C_{max} 72.96 ng/ml; AUCt-∞ 1959.71 ng h/ml; Terminal $t_{1/2}$ 140.69 h; T_{max} 2 h Free Maraviroc: C_{max} 71.67 ng/ml; AUCt-∞ 567.17 ng h/ml; Terminal $t_{1/2}$ 53.23 h; T_{max} 1 h	--	[90]
Nanocrystals					
Cabotegravir	Polysorbate 20 and polyethylene glycol 3500 stabilized nanocrystal	IM/SC	C_{max}(ng/ml) IM 44,900-93,800 SC 33,700-59,700		[105]
Rilpivirine	Poloxmer 338 or D- α-tocopheryl polyethylene glycol 1000 succinate coated nanocrystal (200nm,400nm,800 nm)	IM/SC	***Species: rats*** IM (5 mg/kg): C_{max} 71 ng/ml; T_{max} 7 h; $AUC_{t\text{-}last}$ 3840 ng.h/ml; BA 78 SC (5 mg/ kg): 42; 3; 3540; 72 IM (20 mg/kg): 158; 7; 15300; 78 SC (20 mg/kg): 73; 7; 15500; 78 ***Species: Beagle dog*** IM (5 mg/kg): 619; 0.5; 23200; 102 SC (5 mg/kg): 31.4; 288; 19700; 80 ❖ Pharmacokinetic study in beagle dogs revealed stable plasma concentration (1.4 ng/ml) upto 144 h post SC administration of Rilpivirne nanocrystal (200 nm) compared with 400 nm and 800 nm. Increase in dose (4-fold) led to 2-to 2.7-folds increase in plasma exposure. Upon IM administration, peak plasma concentration was reached in 24 h with rapid decline to 5% of C_{max} while, SC led to constant plasma level (22 ng/ml) until 24 days. Mean exposure by IM and SC being 41.4 μg h/ml and 24.4 μg h/ml respectively. ❖ Higher Cmax with reduced exposure was observed upon increase in particle size of nanocrystal from 200 nm t0 400 nm and 800 nm respectively.	--	[66]
Atazanavir (ATV) and ritonavir (RTV)	Poloxamer 188 stabilized nanocrystals Drug release in MDM cells for RTV peaked at day 1 and sustained until day 10, in contrast to ATV with peak on day 5 with level below 2 mg/ml on day 10 and 15	SC	❖ ATV concentration reached above MEC (150 ng/ml) within 6 weeks while RTV plasma concentration reached 213 ng/ml in 5 weeks ❖ Liver and spleen concentration were relatively constant (1000-10000 ng/g) upto 8 when nanoART was administered every week for 6 weeks	HIV-1_{ADA}intraperitoneally injected in $CD34^{+}$H SC NSG	[159]

(*continued on next page*)

Table 3 (*continued*)

			❖ 100-1000 folds reduction in viral load (VL) upto 2500 copies/ml after 4 weekly injections was obtained with viral rebound upon cessation of therapy after 6 weeks with significant neuroprotective effect	humanized mice	
ATV and RTV (nanoART)	Poloxamer 188 stabilized nanocrystals	SC	After Chronic dose (day 0, and 7) dose (10 mg/kg) SC administration on day 14 the tissue concentration was: ***Species: mice*** *Free ATV*: AUC_{last} (ng.h/ml) 6,164.4; $t_{1/2}$ (h) 253.3; V_{β} (L/kg) 1,933.0; Cl (L/h/Kg) 5.29; $MRT_{0-\infty}$ 120.9 *nanoART-ATV*: 12,592.5; 1,152.5; 1,106.8; 0.67; 171.6 *Free RTV*: 8,028.0; 83.6; 731.4; 6.06; 63.5 *NanART-RTV*: 13,586.4; 230.1; 771.4; 2.32; 142.5 ❖ When nanoART containing ATV and RTV were injected in monkeys, plasma concentration above 100 ng/ml was detected upto 14 days. While in Balb/cJ mice the concentration was 13,41 and 4500-folds higher compared to native drug in plasma, tissue and injection site respectively after single IM dosing.	--	[89]
			❖ Multiple chronic dosing showed 270-folds higher serum and tissue concentration upto 8 weeks		
ATV boosted RTV (ATV/r)	Folic acid functionalized poloxamer 407 stabilized nanocrystals (FA-P407-ATV/r) (FA nanoATV-374±3 nm;0.23±0.01; -14.0±0.6 mV) (FAnanoRTV-390.1±22nm; 0.21±0.01; -6±10 mV)	IM	❖ Plasma concentration in Balb/cJ mice was above MEC for ATV 14 days post administration. Tissue ATV concentration was 37.11- and 3.79-folds higher while, RTV concentration was 3.57- and 1.28-folds higher with FA-P407-ATV/r compared to P407-ATV/r. The bioavailability was 5-folds higher for FA-P407-ATV/r compared to P407-ATV/r ❖ Infected mice depicted restoration of CD4/CD8 ratio in blood and spleen after treatment which was significantly higher compared to control. Also, The HIV p24 content was significantly lower (<2%) when treated with FA-P407-ATV/r compared to P407-ATV/r group.	Hu-PBL intraperitoneally injected in NOD/SCID/IL2R $\gamma c^{-/-}$ mice	[51]
Nanoprodrug					
Myristoylated cabotegravir (MCAB)	Poloxamer 407 stabilized nanocrystals (NMCAB-318±25 nm;0.21±0.02; -22±3.4 mV) (NCAB-315±26 nm;0.28±0.04; -8.2±1.4 mV) (CAB LAP-257±6 nm;0.22±0.02;-23.2±1.7 mV)	IM	***Species: Mice*** CAB LAP: $t_{1/2}$ (h) 71.3±1.2; $AUC_{0-\infty}$ (h ng/mL) 6884479.4±511007.1; $V_{\beta/F}$ (L/Kg) 0.69±0.06 NM CAB: 277.8±5.9; 6897132.5±260736.5; 2.64±0.13 ❖ When administered in male Balb/cJ mice intramuscularly NMCAB was above 4*PA-IC_{90} for 28 days, In male macaques	Hu-PBL reconstituted NSG mice	[11]

(*continued on next page*)

Table 3 (*continued*)

			administration of NMCAB led to 2-4 folds higher $t_{1/2}$ compared to CAB LAP. ❖ The tissue concentration in brain, liver, spleen, lung, lymph node and kidney was above IC_{90}(166 ng/g) n all organs administered with NMCAB compared to CAB LAP ❖ 2090-9-folds and 6.2-folds higher viral suppression was obtained after administration of NMCAB and CAB LAP respectively. $3log_{10}$ higher viral DNA, RNA was obtained after treatment with NMCAB in all tissues after treatment with which correlated with >5 fold increase in Cab concentration.		
Palmitoyl fatty acid conjugated emtricitabine (NMFTC)	Poloxamer 407 stabilized nanoprodrug (350±10 nm;0.24±0.02;-20±0.2 mV;90%)	IM	❖ MDM cell challenged with HIV-1_{ADA} showed 100%and 25% protection after 10 and 15 days post NMFTC treatment. Whereas only 30% protection upto 24 h was obtained after treatment with FTC. ❖ 2-fold and 8-folds higher plasma FTC-triphosphate level was observed in rats after 1 and 7 days post treatment with NMFTC compared with FTC. 2-4 fold higher splenocyte and lymph node concentration of FTC-TP was also observed on day 1& 7 as against FTC group.	--	[63]
Myristoylated Dolutegravir (MDTG)	surfactant stabilized nanoprodrug (309.7±31.7 nm;0.22±0.03;-20.3±1.8 mV)		***Species: rhesus macaque*** ***Λ (h^{-1})*** / ***$t_{1/2}$ (h)*** / ***$AUC_{0-\infty}$ (h ng/mL)*** / ***$V_{\beta/F}$ (L/Kg)*** / CL/F(ml/Kg) / $MRT_{0-\infty}$ DTG: 0.0015±0.001 / 467.1±28.1 / 249,640.2±35.707.7 / ND / ND / 691.7±98.4 MDTG: 0.0016±0.002 / 458.2±55.7 / 41,937.7±16.271.1 / 835.5±334.0 / 1.19±0.36 / 454.6±62.5	--	[161]
Stearoylated Darunavir (NMDRV)	Poloxamer 407 stabilized nanoprodrug (NDRV-384.5±10 nm;0.27±0.01;-7.78±0.36 mV) (NM2DRV-149±2nm;0.26±0.01;-1.74±0.01 mV)	IM	❖ Plasma concentration was above PA-IC90 of 64 ng/ml for 35 days and above 10 ng/ml for 91 days after single IM dose(118 mg/ml) ***Species: male Balb/cJ mice*** ***Concentration (day 28)*** Plasma: NDRV ND / NM2DRV 8.4 ng/ml Spleen: NDRV <3 ng/g / NM2DRV 8216.5±1745.2 ng/g Liver: NDRV ND / NM2DRV 1516.8±217.2 ng/g Lymph node: NDRV <3 ng/g / NM2DRV 26848.7±15689.5 ng/g Brain: NDRV ND / NM2DRV 12.2±3.5 ❖ Amine modified Darunavir prodrug led to no HIV RT activity until 30 days when treated with NMDRV and upon HIV-1_{ADA} challenge in MDM cells as against free DRV showing HIV RT activity from day 5.	--	[138]
Phosphoramidate Lamivudine ProTide (NM23TC)	Folic acid conjugated nanoprodrug (FA-NM3TC)	IM	❖ MDM cells when challenged with HIV-1_{ADA} upto day 30 after treatment with NM23TC for 8h, showed 6.1% and 16%	--	[64,139]

(*continued on next page*)

Table 3 (*continued*)

	(189.5±6.1 nm;0.26±0.01;-21±0.2mV; 72%) In MDM cells M23TC released Lamivudine triphosphate at 1685 ng/ml at day 1 and 229.6 ng/ml at day 30 while, no detectable drug was found in native drug treated cells		❖ breakthrough on day 20 and 30 in contrast to 24h upon treatment with free 3TC. ❖ FA-NM3TC depicted 1.1-folds higher anti-HIV RT activity in MDM cells. ❖ Sustained plasma drug concentration upon IM administration of NM23TC upto 1 month in contrast to 3TC which fell below limit of quantitation in day 7. Spleen and lymph node served as drug depot. ❖ Plasma, liver, spleen and lymph node drug level was 2-folds higher at day 5 and 14 after administration of FA-NM3TC compared to NM3TC.		
Myristoylated Rilpivirine (NM3RPV)	Poloxamer 338 stabilized nanoprodrug (NRPV-277±9nm;0.24±0.02;-9.2±0.3 mV) (NM3RPV-345±5 nm;0.18±0.06;-17.6±0.6 mV)	IM	❖ MDM cells challenged with HIV-1_{ADA} post 8 h after treatment with NM3RPV or NRPV led to >96% protection until 30 days and 67% protection after 10 days t both 10 and 30 μM. ❖ Single IM injection of 45, 75 and 100 mg/kg in male Balb/cJ mice caused sustained plasma level (above PA0IC_{90} 12 ng/ml) until 25 and 7 weeks for NM3RPV and NRPV respectively. 13 and 26-fold increase in plasma half-life and mean residence time (MRT) was obsereved for Nm3RPV compared to NRPV. Spleen, liver and lymph node were substantial depot of M3RPV upto 46 weeks. ❖ In rhesus macaque, IM administration led to 2 to 16-folds higher NM3RPV level compared to NRPV with rectal, lymph node and adipose tissue containing detectable drug upto 204 days	--	[50]
Carbonate and carbamate masking semi-solid emtricitabine prodrug (SSPN)	Polymer coated nnoprodrug (<250 nm;<0.2)	--	❖ PBPK modelling predicted steady plasma concentration for 28 days after reaching C_{max} withing 24h	--	[162]
Abacavir pronucleotide (NM3ABC)	Poloxamer stabilized nanoprodrug (329±3 nm; 0.28±0.01;-45.0±0.4 mV;47.4%) Sustained drug release from MDM cells upto 30 days (100 Fmol/10^6 cells)		❖ Administration of NM3ABC (100μM) led to sustained viral suppression for 15 days , 90% inhibition till day 20 which was reduced to 83% on day 30 when MDM cells were challenged with HIV-2_{ADA}	--	[54]
Polymer and lipid nanoparticles					
Emtricitabine (FTC)	PLGA nanoparticle (FTC-NP) (175.9±24.7 nm; 0.145±0.028; -25.6±1.94 mV; 53.8±5.07%) Drug release at pH 5.5 suggested 62% FTC release in 1 h, therafter constant drug release was obsereved with only upto 85% FTC release on day 30	--	❖ HIV-1 positive TZM-b1 cells treated with FTC-NP depicted 43-folds higher efficacy compared to free FTC. Further, FTC-NP depict similar exogenous HIV-1 inhibition in PBMC compared to free FTC solution.	--	[143]
Bictegravir (BIC)	PLGA nanoparticles (BIC NP) (189.2±3.2 nm;<0.2;-24.3±3.9 mV; 47.9±6.9%)	--	❖ *In vitro* pharmacokinetic revealed 2.4- and 3.1- times higher BIC-NP compared to BIC solution in TZM-b1 cells	--	[144]

(*continued on next page*)

Table 3 (*continued*)

	45% BIC release at pH 5.5 in 1 h after which constant release was observed upto 72% on day 14		❖ BIC NP depict 159 times and 30 times higher efficacy in TZM-b1 and PBCM cells infected with HIVNLX and HIV ADA respectively compared to BIC solution ❖ The selectivity index in TZM-b1 and PBMC was 215,789 and 523.33 for BIC-NP compared to 3.7 and 1.5 respectively.		
Compound 1 (Comp)	PLGA nanoparticle (Comp NP) (370±9.2 nm;<0.2;-28±0.1 mV;95±9.1-104±26.2%)	Intra-periotneal (IP)	***Species: Balb c/J mice*** ***AUC0-last (μg.h/mL)*** / ***CL, ml/min/kg*** Comp (20 mg/kg): 209.2±23.8 / 1.5 Comp NP (20 mg/kg): 472.9±20.99 / 0.7 ❖ Complete inhibition of HIV-1 infected TZM-b1 cells was observed upto day 35 when treated with Comp NP as against 4 h for Comp 1 ❖ Intraperitoneal administration of Comp NP led to 100-fold greater plasma concentration compared to EC_{50} for WT HIV-1. ❖ Upon injection of compound 1 (100 mg/kg) and comp NP (190 mg/kg) intraperitoneally in HIV-1 infected humanized NOD.*Cg*-Prkdc^{SCID}Il2rg^{tm1wjl}/*Szj* mice depicted 10^4 plasma viral load on day 8 in compound 1 group and no VL upto 19 days in Comp NP group with increase to 10^4 and 10^5 on day 25 and 32.	HIV-1 infected humanized NOD.*Cg*-Prkdc^{SCID}Il2rg^{tm1wjl}/*Szj* mice	[94,163]
Elvitegravir (EVG)+ tenofovir alfenamide (TAF)+emtricitabine (FTC)	PLGA nanoparticles (PLGA cARV NP) (243.2±5.8 nm;<0.2;-20.73±9.3 mV;38.6±2.9%(EVG),50.7±2.6 (TAF), 46.4±3.6 (FTC))	SC	❖ Plasma viral load was undetectable after third biweekly dose of cARV NP administered SC with detectable concentration of each drug in lymph node and female reproductive tract at week 22.	Humanized BLT mice	[95]
TAF+EVF	PLGA nanoparticles (TAF+EVG NP) (190.2±1.7 nm;0.14±0.01;-19.2±1.7 mV;54.1±3.6% (TAF), 44.6±2.4% (EVG))	SC	***Species:Hu-CD34-NSG mice*** ***$AUC_{0\text{-}lastconcn}$ (μg.h/mL)*** / ***$t_{1/2}$*** TAF: 14.1±2.0 / 14.2 h TAF-NP: 23.11±4.4 / 5.1 days EVG: 7.2±0.8 / 10.8 h EVG-NP: 39.7±6.7 / 3.3 days ❖ Vaginal AUC was 2.7-3.9 folds higher for TFV and EVG compared to the vaginal AUC when in solution. ❖ TAF+EVG NP depicted 390-folds increased potency compared to TAF and EVG solution ❖ When mice treated with TAF+EVG NP were challenged with HIV-1, 100% viral protection was observed at day 4 and at day 14, 60% protection was elicited	NOD/SCID/IL2rg null, CD34-NSG mice	[52,145]
TAF and FTC	PLGA nanoparticles (TAF+FTC NP) (233.2±12.8 nm; 0.11±0.05; -19.1±4.1 mV;69.2±14.5 (TAF),65.9±18.2 (FTC))	SC	***Species: Hu-CD34-NSG mice Plasma*** ***C_{max} (ng/mL)*** / ***AUC_{all} (Day.μg/mL)*** / ***CL (L/day/kg)*** / ***V_d (L/Kg)*** / ***$t_{1/2}$ (h)*** / ***MRT_{last} (h)***	Hu-CD34-NSG mice	[53]

(*continued on next page*)

Table 3 (*continued*)

	Drug release in endosomal pH revealed 73% total TAF and FTC release within 30 min with effective time constant of 22.6 and 15 min respectively.		TAF	942±137	0.6±0.08	33.50	285.3	14.2	13.4
			TAF-NP	15,954±2716*	2.5±0.4	78.7	145.6	30.8	13.5
			FTC	850±242	0.2±0.05	1031	149.3	2.4	5.9
			FTC-NP	34,026±3140*	3.9±0.8	49.7	204.3	68.4	13.5
			Vagina						
			TAF	4.0±1.1	2.2±0.4	92,448	39,558	6.5	10.0
			TAF-NP	58.4±23.4*	10.9±2.1	18,345	46,675	42.3	26.3
			FTC	4.5±1.0	1.6±0.4	118,762	91,640	12.8	11.2
			FTC-NP	54.1±13.2*	5.4±1.1	35,791	256,605	119.3	13.6
			*-p<0.05 compared with free drug solution						
			❖ 80% protection was obtained upon challenging hu-CD34-NSG mice with HIV-1 on day 4 after treatment with TAF+FTC NP at day 0, while it reduced to 60% on day 7 and 14.						
ATV, RTV and Tenfovir (TFV)	DSPC and DSPE-mPEG2000 (DcNP) (6-62 nm;99±8.2% (ATV),92±7.1% (RTV),10±0.8% (TFV))	SC	❖ Sustained drug concentration upto 336 h was obtained for ATV, RTV and TFV in plasma and upto 336 h and 192 h for ATV,RTV and TFV respectively in PBMC upon DcNP administration compared to free drug wherein drug concentration lasted for 48h after SC administration in macaque.						[91]
			❖ The AUC was 5 and 35 folds higher and Clearance was 4- and 23-folds lower for ATV and TFV respectively, $t_{1/2}$ was 110-,17- and 7-fold higher for ATV, RTV and TFV respectively when DCNP was administered SC compare to free drug.The lymph node mononuclear cells showed 3-fold higher concentration of ATV and RTV when administered through DcNP compared to free drug.						
			❖ MBPK modelling depicts slower lymphatic passage for ATV and RTV compared to TFV. Also, it predicted 2 week dosing interval in macaque depicting long acting potential.						
TFV, RTV and Lopinavir (LPV)	DSPC and DSPE-mPEG2000 (TLC-ART 101 LPV)	SC	❖ SC administration of TLC-ART-101 LPV in Macaque led to sustained plasma level upto 336 h. Details are as below:						[12]
			Species: Rhesus macaque	***$AUC_{0-24\ h}$ (h*μg/mL) (mean± %CV)***	***$t_{1/2}$ (h) (mean± %CV)***	***CL/F (L/h/Kg) (mean± %CV)***	***$MBRT_{0-24\ h}$ (h) (mean± %CV)***		
			LPV	4.35±7	8.65±28	4.64±14	10.83±5		
			RTV	1.37±9	7.99±38	4.23±15	10.78±5		
			TFV	14.4±4	8.01±51	0.72±4	2.61±12		
			TLC-ART 101 LPV						
			LPV	10.98±48	476.94±173	0.85±85	116.09±8		
			RTV	4.80±57	44.06±46	1.43±56	24.86±9		
			TFV	416.55±15	65.33±11	0.02±15	102.68±7		

(*continued on next page*)

Table 3 (*continued*)

			❖ MBPK modelling was applied to predict the various pathways which LPV RTV and TFV would follow which included fast, intermediate and slow lymphatic pathway. Model predicted lag time of 0.1-2.2h, 10.9-38.8 h and 122.1-262.2 h for fast, intermediate and slow lymphatic pathway. Based upon the lag time LPV and RTV followed slow and fast lymphatic pathway respectively while, TFV was available for all three when TLC-ART 101 LPV will be administered via SC.		
ATV, RTV and Efavirenz (EFV)	$mPEG_{2000}$ DSPE (ATV+RTV+EFV nanoART) (281-470 nm;0.200-0.288;-31.6--13.5 mV)	SC	❖ Upon treatment with ATV+RTV+EFV nanoART after 12 h of infection with HIV-1_{ADA} in NSG mice, ATV and RTV level was above MEC for ATV and RTV in humans (150 ng/ml) on day 14, but the EFV concentration was 4-6 folds lower compared to its MEC. ❖ HIV-1 p24 was significantly decreased in blood when treated with ATV+RTV+TFV nanoART compared to ATV+RTV treatment. The viral gene level was decreased by 3-order of magnitude upon treatment with ATV+RTV+EFV nanoART compared with 2-order of magnitude when treated with ATV+RTV	HIV-1_{ADA}infected PBL-NSG mice	[137]
ATV, RTV and TFV	DSPC and DSPE $mPEG_{2000}$ lipid drug nanoparticle (LDN) (63.6±1.1 nm;85.5±8.2% (ATV),85.1±7.1% (RTV), 6.1±0.8% (TFV)) ATV showed pH dependent release with almost 100% drug release within 24 h at pH 3.	SC	❖ SC administration of ATV (25 mg/kg), RTV (12.8 mg/kg) and TFV (15.3 mg/kg) led to sustained plasma concentration upto 7 days in primates.Only 20% of total AUV was attributed to early phase (0-8h) for all 3 drugs.	--	[65]
LPV, RTV and TFV	DSPC and DSPE $mPEG_{2000}$ lipid nanoparticle (LNN) (52.4±9.1 nm;93.6±5.5% (LPV),90.7±7.4% (RTV),11.9±3.0% (TFV))	SC	***Species: macaque*** ***AUC_{0-168h} (μg.h/mL)*** LPV 3.83±4.04 RTV 1.39±1.18 TFV 56.6±17.04 ***LNN*** LPV 69.6±10.7 RTV 19.4±12.2 TFV 395.0±344.5 ❖ LNP administered in four macaque revealed 50-folds higher intracellular concentration in lymph nodes compared with free LPV, RTV and TFV respectively. LPV, RTV and TFV plasma concentration were sustained upto 7 days compared with free drugs.	--	[92,93]

Values in round bracket indicate particle size; polydispersity index; zeta potential; % entrapment efficiency.
nm-nanometer and mV- millivolt; BA-bioavailiability

enhanced solubilization and drug loading [147–149]. Moreover, lipids are biocompatible, biodegradable [150] and hydrophobic, which could facilitate the intracellular delivery of drugs [151]. LNP can form depot after SC or IM administration, whereby it circumvent blood circulation and enter into the lymphatic system to target HIV residence and spread-sites located in multiple regions [152] by using reduced dose and small injection volume [79]. Furthermore, cARV with differential physico-chemical properties can be encapsulated into lipid nanocarriers. Therefore, a targeted long-acting antiretroviral product 101 (TLC-ART 101 LPV) was designed by incorporating Lopinavir (LPV), Ritonavir (RTV), and hydrophilic Tenofovir (TFV) into DSPC and DSPE-PEG nanocarriers for lymphocyte targeting in non-human primates (NHP)

[12]. Improved pharmacokinetic profile with enhanced $AUC_{0-\infty}$ by 2.5, 3.5, and 28-folds for LPV, RTV, and TFV respectively upon TLC-ART101 LPV subcutaneous administration was obtained compared with free drug solution in the macaque. Also, the half-life of TLC-ART101 LPV was prolonged by 55.1, 5.1, and 8.2-folds for LPV, RTV, and TFV, respectively. Further, plasma concentration-time profile of each drug showed short, medium and long lag time represented as 3-waves, which was predicted due to the entrapment of nanoparticles into lymph nodes, slow drainage from thoracic lymph vessels into blood circulation and drug release from lymphocytes (a secondary depot) [12]. Further, to explore the application of TLC-ART technology, LPV was replaced with second-generation protease inhibitor (atazanavir, ATV). The TLC-ART incorporating ATV, RTV, and TFV combination (ATV-RTV-TFV DcNP) depicted sustained plasma level until 336 h post-SC administration in macaque compared with 48 h when in solution. Enhanced targeting of ATV-RTV-TFV DcNP to PBMC was confirmed with higher AUC_{PBMC} by 33.46-, 1.5, and 5-folds for ATV, RTV, and TFV, respectively, when compared with drug solution [91]. Nevertheless, biodistribution, efficacy, and toxicity profile of LA lipid-based nanoformulations are yet to be established to enable successful translation from lab to clinic.

3.2.6. Long-acting aspherical nanoparticles

Aspherical nanoparticles have become enticing revealing a new arena of research with respect to longer circulation time and escape of phagocytosis [153–155]. It has been identified that the angle between macrophage and aspherical nanoparticle during interaction determines its internalization. If the tangent angle is $\leq 45^{\circ}C$, the particle gets internalized [156]. Further, it was observed that the higher the surface area of nanoparticles higher is the attachment to macrophages [157]. Thus, prolate ellipsoid attaches more compared to oblate aspherical followed by spherical nanoparticles. Furthermore, the internalization of oblate ellipsoid was found to be greater compared to the sphere with the least internalization of prolate ellipsoids [158]. For instance, LA NMCAB nanoformulations was phagocytosed 60-folds higher compared to CAB LAP due to presence of oblate ellipsoids along with rod shaped nanocrystals in MDM cells. The NMCAB nanocrystals were visible in macrophages even after 8 h, depicting the formation of macrophage depot and prolonged half-life of 54 days. [11]. In contrast, rod-shaped and rectangular-shaped ATV and RTV nanocrystals, respectively, were utilized for higher attachment onto macrophages leading to long term macrophage retention. The ATV and RTV nanocrystals (nanoART) were developed by high-pressure homogenization using Poloxamer 188 as a stabilizer. The drug release studies of aspherical nanocrystals in human monocyte-derived macrophage (MDM) cells depicted sustained drug release for ATV and RTV up to 15 days. Further, multiple weekly dose administration in NSG mice up to 6 weeks elucidated plasma concentration of 183 ng/ml and 213 ng/ml by week 6 (ATV) and week 5 (RTV), respectively. Cessation of dosing led to a decrease in plasma concentration, but tissue concentration remained constant from 1000-10000 ng/ml. HIV infected NSG mice, when treated with nanoART showed significant retention of $CD3^{+}CD4^{+}$ count compared to the control group. After four injections, 100 to 1000-fold reduction was observed in the viral level. However, viral rebound was observed upon treatment cessation after six weeks. The lymph node size was reduced by 50% in the untreated group compared with the treatment group, and the lymphoid organ led to viral relapse upon treatment cessation, which indicated the need for sustained weekly administration. The nanoART increased the expression of microtubule-associated protein 2 (MAP2+). The brain morphology was retained in the nanoART treatment group compared with untreated mice. Thus, nanoART can be utilized as maintenance therapy provided drug resistance is kept in check as indicated by viral rebound upon cessation of therapy [159]. In contrast, attack on the major axis may lead to complete phagocytosis of elongated rod-shaped nanoparticles making their depot inside macrophages [156]. In this regard, lipid-coated rilpivirine-bismuth sulfide nanorods (BSNR-RPV) similar to RPV nanocrystals (NRPV) depicted MDM uptake and similar antiretroviral property (> 98%) when compared with rilpivirine nanocrystal. The LuBSNR nanoparticles were transitioned from liver to spleen, later in gut, and spleen in 120 h. Further, the presence of LuBSNR in the marginal area of spleen confirmed uptake of nanorods by macrophages [160].

4. Physiology-based pharmacokinetic (PBPK) and mechanism-based pharmacokinetic (MBPK) modeling: a tool for long-acting antiretroviral nanoformulation synthesis

PBPK modeling has become more alluring due to its ability to predict tissue/plasma partition coefficient based on drug-specific *in vitro* and *in silico* data, which has played a critical role in the development of LA nanoformulations. PBPK modelling is vital in the development of LA ARV nanoformulations administered to HIV infected population with abnormal physiology like changes in immune cell level, changes in tissue morphology as well as changes associated with other secondary infections. The PBPK models are based on the principle that total drug concentration in all the tissues is in equilibrium with the total drug concentration in plasma, considering kidney and liver as eliminating organs [18]. The PBPK modelling involves four steps as follows [18,19]:

(i) Developing a general model containing various compartments (organs/tissues) wherein biodistribution is expected to occur which is connected to central compartment (circulatory system). It may involve a lumping approach wherein organs of similar physiological, physicochemical, and biochemical properties are lumped together, (ii) Division of every organ into various compartments based on the type of model viz; perfusion limited or permeability limited, (iii) Developing various algebraic equations for static process for each tissue compartment and (iv) Determination of physiology and drug-specific parameters for developed PBPK model.

PBPK model could be applied to determine the clinical pharmacokinetics and dose of LA nanoformulation. For instance, Rajoli et al. used the PBPK model to optimize the IM LA nanoformulations of eight antiretrovirals drugs including tenofovir, emtricitabine, etravirine, rilpivirine, efavirenz, dolutegravir, raltegravir and atazanavir. The compartmentalization was based on three hypotheses viz; the compartments were considered well stirred with the instant distribution of drugs, drugs are not absorbed through the colon, and the model is limited to blood flow. The permissible deviation from predicted values was restricted to 0.5-folds. The predicted LA PK parameters were obtained from clinically available data of oral formulations with multiple dosing of ARV. The dose limit was kept to 1500 mg. The prediction of pharmacokinetics and dose was optimized for the IM route such that the plasma concentration shall remain at IC_{95} and IC_{90} for protein-bound and unbound drugs, respectively, at C_{trough}. The validation of the PBPK model was done against existing clinical data for oral SR rilpivirine formulation. For IM administration, the IM depot was added as a separate compartment. The model was considered validated if the mean AUC for the predicted LA IM depot was ± 50% of the available clinical data. The model predicted that tenofovir, emtricitabine, efavirenz and rilpivirine LA nanoformulation could be administered as a monthly depot. Due to the physicochemical properties of dolutegravir LA, it was considered to be administered at the lowest dose (105 mg) for months. Raltegravir LA(800 mg) and atazanavir LA(600 mg) were suitable as monthly and weekly administration, respectively. Oral loading dose for all ARV except tenofovir and emtricitabine was suggested, considering the lag time of 24 h in case of LA ARV nanoformulations to reach effective plasma concentration. The model suggested the administration of two simultaneous LA formulation by the IM route [164]. However, the PBPK model did not consider gender-specific physiological and anatomical differences and stability of LA nanoformulation over the time.

Administration of LA nanoformulations to children and adults is generally avoided mainly due to toxicity and adverse drug reactions associated with it. Therefore, PBPK modeling could be a promising

approach to predict the dose of LA nanoformulations before clinical trials. For instance, Rajoli et al. developed the PBPK model to predict the dose of LA nanoformulation of rilpivirine and cabotegravir considering physicochemical properties of rilpivirine and cabotegravir, clinical data obtained from 100 virtual adults and LATTE-2 trial as input variables. Dose was predicted, considering the concentration of cabotegravir and rilpivirine would remain above the C_{trough} of 1.35 μg/ml and 70 ng/ml for both the drugs respectively for 52 weeks. Further, a differential sensitivity analysis was done by determining the change in plasma concentration for change in blood/plasma ratio, cardiac output, plasma clearance, liver weight, fraction unbound, and release rate. It was observed that the predicted AUC was +13.2 and +15.6%, C_{max} was -6.5%, and +6.1%, C_{trough} was +8.8 and 9.1% for rilpivirine and cabotegravir respectively against obtained clinical data. Further, plasma drug concentration of cabotegravir was sensitive to only cardiac output and systemic clearance suggesting the higher impact of UDP-glucoronosyltransferase in drug elimination. The model suggested rilpivirine oral dose for four weeks of 25 mg followed by loading dose on body weight basis of 250-550 mg (15-70 kg) and maintenance dose of 200-500 mg for rilpivirine LA. For cabotegravir,10 mg (14-50 kg) and 20 mg (50-70 kg) oral dose based on body weight, followed by 200-600 mg and 100-250 mg loading and maintenance dose for all body weights in children and adults which can maintain the plasma concentration above IC_{90} of each drug. Therefore, prediction of dose and PK of LA nanoformulations majorly depends upon physicochemical properties and ADME of the drugs [165]. A microneedle array patch of LA cabotegravir and rilpivirine was also developed with the aid of PBPK modeling for once-a-week use. The modeling was based on the assumptions viz; drug diffusion from stratum corneum to blood circulation is unidirectional, the hair follicles covers 0.1% of entire skin area, diffusion, partition coefficient and release rate of the drug from nanoparticles into the skin would be constant and only the drug can diffuse through the layers of the skin. It was predicted that equivalent C_{trough} was achieved when loading dose of cabotegravir and rilpivirine was 360 mg and 270 mg, respectively, with 180 mg of maintenance dose of both the drugs after IM administration [166]. Due to the change in physiological parameters including a decrease in height, weight, decrease in migratory motor complex, changes in liver microsomal enzymes, decrease in organ size, and decrease in cardiac output affecting blood flow to various organs with age, LA nanoformulations have not been attempted for the elderly population. These factors should be taken into account while the prediction of dose and pharmacokinetics of LA ARV nanoformulations in geriatrics [167].

In contrast to PBPK modeling, MBPK modeling also considers certain processes including target site distribution, target binding and activation, signal transduction, disease process and progression during elicitation of pharmacological effects. These processes depend upon the properties related to the drug and biological system. Drug-related properties including *in vivo* binding and efficacy, could be predicted and scaled up based on the *in vitro* bioassay data. In contrast, the pharmacodynamic properties mainly depend upon the species, remain almost constant and hence need not to be scaled up. However, biological system-related processes, including protein expressions and the rate constant during expression of the proteins required for drug-receptor binding, could be obtained from *in vivo* data after scale-up for the desired species [168]. Moreover, the prediction of plasma concentration does not always confirm the site-specific distribution of the drug due to the involvement of various transporters, which may synergize or antagonize the effect of the drug. Therefore, it may include receptor-based theory, which considers target site-specific and receptor concentration to obtain the desired response [20].

Recently, kraft et al. developed long-acting drug combination nanoparticle (TLC- ART101) incorporating lopinavir (LPV), ritonavir (RTV) and tenofovir (TFV) for enhanced retention in lymph nodes. The TLC-ART101 were subcutaneously administered to macaque, and the data obtained were used for the MBPK modeling [168] of TLC-ART101. One compartment model with first-order absorption, in the case of LPV and RTV and two-compartment model with first-order absorption for TFV were applied during modeling. The model was based on the assumption that nanoparticles were taken up by the lymphocytes, trapped into lymph sinuses and traverse through the lymphatic vesicles, draining slowly into systemic circulation due to larger intercellular fenestration (100 nm) while, free drug enter the systemic circulation through smaller intercellular space (8-12 nm) after subcutaneous administration. Further, 100% of LPV and RTV loaded nanoparticles were taken by the lymphatic system while only 10% TFV reached lymphatic vessels, as 90% TFV was bound onto the surface of the nanoparticles. Additionally, it was also assumed that the nanoparticles remained stable at the subcutaneous site and did not allow any drug release at the injection site. Based on these assumptions, the composite compartment model was developed (Fig. 3A). The compartments were based on the fast, intermediate, and slow rate of transit of the nanoparticles into the lymphatic system after subcutaneous administration. It was observed that LPV was more available for slow lymphatic transit of nanoparticles called as slow lymphatic compartment as compared to RTV. While, TFV was equally available in all the compartments. The differential distribution into three lymphatic compartments of the individual drug from TLC-ART101 was attributed to the non-uniform distribution of the specific drug in nanoparticles and different metabolism/anabolism of individual drugs in lymphocytes. The plasma concentration-time profile obtained after MBPK modeling is depicted in Fig. 3B. Further, prediction of lymphatic exposure by the MBPK model for each drug was found to be 80% LPV exposure for two weeks, 100% RTV would be exposed within 96 h, and TFV release was faster than LPV in lymphatic. Therefore, MBPK modeling could successfully account for the three different pathways of the lymphatic system as the mechanism for multiphasic waves in plasma concentration of ART upon administration of LA nanoformulation. Further, the author hypothesized the role of tissue lipases and high endothelial venules in lymph nodes along with acid and base stable property of LPV and RTV, leading to their endosomal and lysosomal release as reason for three different lymphatic pathways depicted in present MBPK modeling [12]. The role of PBPK and MBPK modelling for determination of LA nanoformulation clinical pharmacokinetic has been elaborated in Fig. 4

5. Animal models used for evaluation of *in vivo* efficacy of long-acting antiretroviral nanoformulations

The relapse of HIV is a common phenomenon due to the occurrence of latent provirus into tissues and organs, which regain their infection potential upon interruption of ARV [22]. In order to elucidate the mechanism of relapse and develop ARV treatment against the latent phase for humans, efficient preclinical models should be established. The humanized mice model and NHP have been developed to mimic the disease progression due to HIV in humans.

5.1. Humanized mice model

Development of *in vivo* models mimicking HIV infection, transmission, and prophylaxis in small rodents was essential for preclinical studies, considering the existence of HIV in only minuscule species viz; humans (pathogenic) and chimpanzee (non-pathogenic) [23]. NHP are an alternative to humans. However, ethical constraints associated with the use of NHP during preclinical studies of formulations is a major limitation. Therefore, immunocompromised rodents with human engraftment were developed as *in vivo* models for evaluation of the efficacy of antiretroviral drug formulations [24]. Humanized mice models have been developed by transplantation of 1) single or many transgenes from humans into wild type mice, 2) Normal or diseased human cells/tissues into immunodeficient mice, 3) $CD34^+$ hematopoietic stem/progenitor cells (HSPC) into mice or combination of all three types [24]. HIV pathophysiology could be successfully replicated in

humanized mice including $CD4^+$ and $CD8^+$ T cell depletion, upregulation of programmed cell death proteins, rectal and vaginal transmission and gastrointestinal viral colocalization [25]. For instance, systemic viral persistence with the faster doubling of $CD4^+$ and $CD8^+$ T cells in the thymic organ was obtained in human liver/thymus implanted severe combined immunodeficiency mice (SCID mice). However, the infected T cells were found only in thyroid organs, which requires surgical exposure of other tissues for HIV infection [26]. In order to enhance the peripheral blood immune cells, Hu-PBL SCID was developed wherein human-derived peripheral blood lymphocytes were administered intraperitoneally in SCID mice. However, the educated T-cells from the host proliferate and recognize mice cells as foreign after some time, generating host-graft rejection, leading to the use of Hu Thy/Liv SCID and Hu-PBL SCID models for short term studies [25]. For instance, the humanized SCID mice model could be utilized to evaluate pharmacokinetics, biodistribution and efficacy of single-dose LA nanoformulations [163]. The use of this model for evaluation of LA nanoformulations after multiple dosing for longer duration with reduced dosing frequency may cause erroneous results. In contrast, implantation of Thymus/liver tissue in NOD/SCID common gamma chain knockout (Hu Thy/Liv NSG) mice were developed to increase the level of systemic and peripheral T-cells due to extended engraftments of human immune system along with suppressed gene which produces mice immune cells. The NSG mice maintain a high level of viremia in peripheral blood and tissues, and shows viral rebound upon cessation of ART as observed in humans. This model is specifically useful to evaluate drugs/drug products specifically targeting T cells as they lack antigen presenting cells [169]. Therefore, this model could be utilized for the evaluation of LA nanoformulations, targeting to T-lymphocytes to develop secondary depot [12]. Moreover, double knock out (DKO) mice are injected with $CD34^+$ HSPC which is sensitive to viral replication upon infection intravenously or intravaginally and could be used for identification of drug resistant strain. DKO mice showed the presence of T cells, B-lymphocytes, natural killer cells, and dendritic cells in all organs. However, limited T cells were observed in the female reproductive tract and intestine [24]. Bone marrow-liver-thymus (BLT) mice is another DKO subtype consisting of bone marrow engraftment in addition to fetal thymus and liver derived $CD34^+$ engraftment, which leads to the development of lymphocytes, NK cells, monocytes, macrophages and dendritic cells throughout the body. Further, it encompasses $CD4^+$ and $CD8^+$ T lymphocytes specific to gut and female reproductive tract [24]. BLT mice are known to produce extensive human immune responses amongst all humanized mice models. Therefore, this model can be used for evaluation of LA nanoformulation for PrEP treatment [170].

Macrophages are major residence sites for HIV and are known to engulf HIV infected T-cells. In order to confirm the ability of developed nanoformulations to target macrophages in absence of T-cells, $CD34^+$ hematopoietic stem cells were transplanted into T-cell deficient NOD/SCID mice to generate Myeloid only mice (MoM) [171]. However, this model lacks the human thymic microenvironment and human leucocyte antigen, thereby losing the ability for a robust immune response [24]. In order to improve the immune response in humanized mice models that depict ineffective human lymphocytes and NK cells in NOG/NOD/BLT, exogenous factors like interleukins were added into developed models to enhance humanization [24]. For instance, NOD.*Cg-Prkdc*^{scid}*IL2rg*^{tm1Wjl} NSG mice are the best available model with the highest human stem cell (HSC) compatibility due to both SCID and interleukin-2 gamma chain mutation, which cannot produce T-cell, B-cell and NK by themselves. At the same time, they replicate the cells of human origin when transplanted within them [172]. These models have been widely developed to study the effect of formulations on the progression of neurological complications associated with AIDS [169]. For instance, LA ATV and RTV nanocrystal suspension were evaluated for its neuroprotective effect in humanized NOD/scid-IL-2Rg$_c^{null}$ mice which showed increased microtubule-associated protein 2, neurofilament expression and synaptophysin after 6 injections, administered at a frequency of once in a week [159]. Further, a combination of each model with gene suppression leads to exact mimicking of disease and hypothesized treatment making it feasible to study the effect of LA nanoformulations for single and multiple dosing as well as to evaluate LA nanoformulations for PrEP [52,53]. For instance, The NOD/shi-scid/γc null (NOG) mice with transplanted $CD34^+$ derived from the blood of umbilical cord and knocked IL2 gene when challenged with CCR5 and CXCR-4 sensitive HIV strain depicted high level of viral transmission and $CD4^+$T cell depletion as in HIV infected humans. LA SC

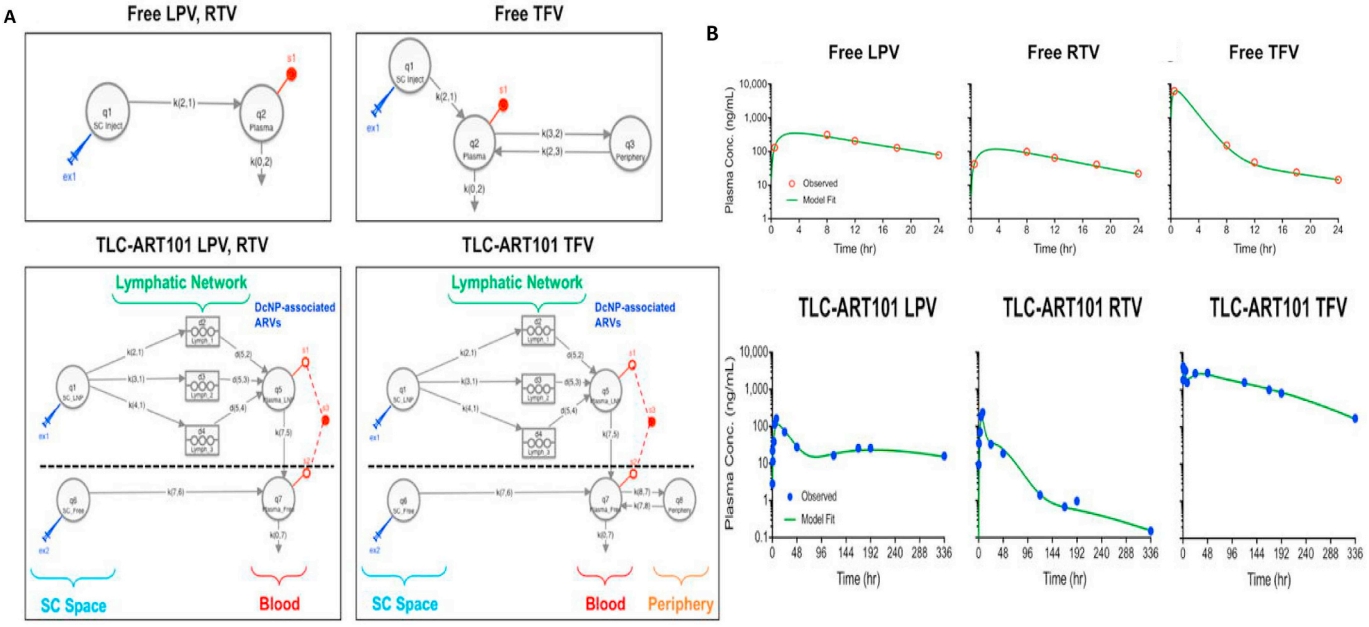

Fig. 3. Mechanism-based pharmacokinetic modelling (A) Representation of mechanism-based compartmentalization for free drug disposition into circulatory system and TLC-ART101 disposition into circulatory system preceeded through lymphatic system. (B) MBPK model (curves) fitting to observed plasma concentration for LPV, RTV and TFV after single SC dosing of free LPV, RTV, TFV and TLC ART 101 in macaques (n = 8) [12].

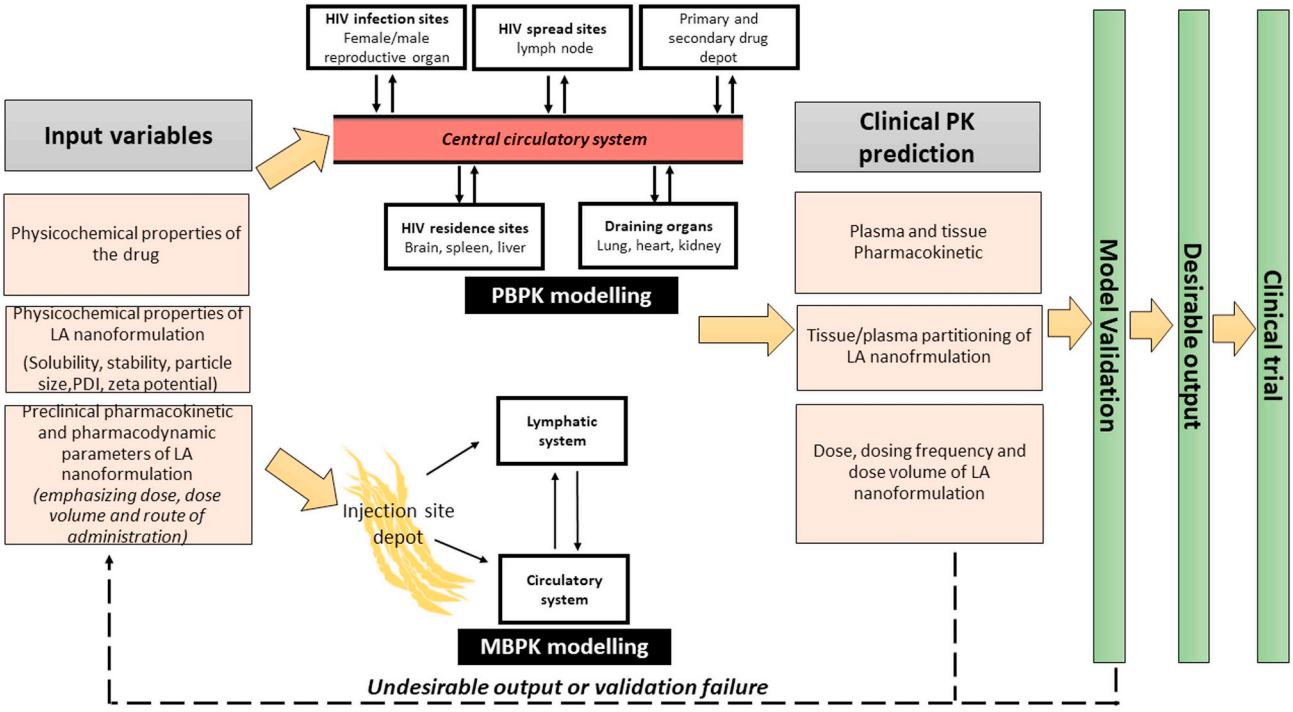

Fig. 4. Application of pharmacokinetic-modelling in development of long-acting antiretroviral nanoformulation

administration of TMC278 (NNRTI in the late-stage clinical trial) and TMC 181(early-stage pre-clinical trial protease inhibitor) depicted above target plasma concentration up to 14 and 7 days respectively. Further, the infected mice, when treated with daily oral regimen of tenfovir disproxil fumarate (TDF) and 3TC, along with once-weekly SC dosing of TMC278 LA depicted 79% decline in viral RNA level. Rest of the 21% mice experiencing failure in viral suppression showed viral mutation, including M1841 (3TC) and E138K (TMC278 LA) as identified in humans previously. While, oral once-weekly dosing of AZT, RTV and 3TC and TMC278 LA monotherapy caused wasting symptoms and breakthrough in viral load. But, the viral load was maintained below limit of detection when both TMC 278 LA and TMC 181 LA were used as maintenance therapy (until 99 days) in mice with already low viral RNA after treatment with oral TDF, 3TC, TMC278LA and TMC181 LA for 44 days [173]. Therefore, based on the targeting potential of developed LA nanoformulation, different humanized mice models have been reported to study pharmacokinetics, biodistribution, and efficacy.

5.2. Non-human primates

NHP is considered an appropriate *in vivo model* to evaluate the antiretroviral efficacy of drug/formulation due to their phylogenetic similarity with humans. Many African macaques are the host for simian immunodeficiency virus (SIV) however, they do not show disease pathogenesis. Only two species, namely, SIVsmm infected *Sooty magabey,* and SIVagm in African green monkeys, which depict HIV-2 in humans and SIVmac in macaques, have been identified to be pathogenic [174]. Therefore, Asian macaques infected with SIV were developed as an *in vivo* model for HIV, which showed disease induction and progression similar to HIV-1 infection in humans. Three different Asian macaques, namely, rhesus macaque, pig-tailed macaque, and cynomegalous macaque, are available as *in vivo* models [175]. However, the selection of NHP amongst the available ones is critical and depends upon the availability, cost, and duration for disease induction and progression. For instance, cyomegalous macaques are rarely used species due to their incomplete adaptation to infecting viruses compared to rhesus and pig-tailed macaques, which require 1-2 years and 42 weeks respectively for disease induction and progression [176].

The NHP could be infected with various lentivirus mimicking HIV, including SIV, SHIV, and its variants. SIV and HIV have many similarities including similar rate and target cells for transmission, transcription of viral long term repeat chain to maintain viral DNA upon exposure to interferon, similar stimulatory signals for converting SIV and HIV into latent phase, uniform distribution in peripheral blood, lymph node and mucosal sites as in HIV, similar reservoir and slow clearance of infected cells due to mutation [174]. Therefore, SIV is preferred due to rejection of HIV-1 direct infection by TRIM5α, apolipoprotein B-editing catalytic subunit like 3 (APOBEC3), and Tetherin in macaques [177]. However, SIV is accompanied with drawbacks including only 53% nucleotide identity between HIV and SIV [176], infection of SIV only in monocytes and macrophages as against T cells which are the major target of HIV and different host factors (origin of the virus, major histocompatibility-I alleles and restriction allele) [177]. SIVmac251, SIV239, SSIVsmE543-3 and SIVsmE660 are widely used SIV for generation of HIV-1 like symptoms [178]. SIV utilizes CCR5 co-receptor for viral transmission like HIV, but it contains viral *env,* which is resistant to neutralizing antibodies. On the contrary, few SIV strains, including SSIVsmE543-3 and SIVsmE660 are sensitive to TRIM5 protein and therefore inhibit viral transmission and are ineffective when treated with many ARV [176]. The lacunae of SIV are overcome by chimeric SHIV which uses CXCR4 co-receptor like HIV-1 [179]. SHIV expressing HIV-1 *env* are developed by replacing genes for envelop proteins with the HIV-1 gene for envelop proteins like *rev, tat, vpu, and env* gene [176]. Multiple passage of SHIV in macaques leads to HIV progression with drastic depletion of $CD4^+$ T lymphocytes within three months. Unlike SIV, which infects $CCR5^+$ lymphocytes causing depletion of memory T cells, SHIV infects $CXCR4^+CCR5^-$ and causes peripheral blood and lymph node naïve $CD4^+$T cell depletion. SHIVSF162P3 strains majorly adapted to rhesus macaques were developed to evaluate the viral transmission failure upon microbicides treatment [176]. Therefore, SHIV and SIV infected rhesus macaque could be utilized to evaluate efficacy of PrEP LA nanofrmulations

[107,108]. In order to enhance the strain susceptibility to non-nucleoside reverse transcriptase inhibitors, SHIV HIV-1 *pol* were developed by transferring HIV-1 RT polymerase (pol) into SIV. Further, an effort to engineer exact HIV replica in macaques HIV-1_{vif} gene was replaced with SIV_{vif} mac to develop stHIV which is resistant to APOBEC-3 gene and replicate in pig-tailed macaque similar to humans [176]. Therefore, successful *in vivo* model could be developed by infecting NHP with available viral strains mimicking HIV (Table 3).

6. Long-acting antiretroviral nanoformulations: challenges and future perspective

The LA effect of nanoformulation grounds on their established physicochemical properties. Retention of these physicochemical properties during the translation from lab to clinic with continuous manufacturing process remains elusive [180]. LA nanoformulation demands the ability to incorporate drugs with different physicochemical properties using single platform technology for its clinical application. However, differential drug release of the ARV [12], drug-drug interaction, and felicity of common carrier remains major defiance [16]. Techniques to establish sterility of LA nanoformulation to maintain equipoise with its stability during manufacturing and storage are yet to be established [181]. Moreover, although the secondary immune cell depot causes long-acting effect, toxic metabolites when LA nanocarriers are directed towards cellular endosome with acidic pH needs to be thoroughly investigated along with tissue and plasma pharmacokinetic and biodistribution. Nanosuspension, specifically, nanocrystals tend to cause ostwald ripening and depict polymorphism [75], affecting their solubility and *in vivo* performance, which until now have not been studied for LA nanoformulations. Additionally, the majority of ARV are administered in higher doses, making them unsuitable for LA nanoformulations due to issues regarding dose-volume [15], syringeability, stability, and depot consistency. A standard platform technology may aid in the presentation of cART to individuals with distinct physiology establishing horizon for personalized regimen inhibiting drug resistance [13,57]. A combination of substantial modification in the viral genome along with a long-acting cART regimen may serve as an excellent remedy in complete eradication of chronic HIV infection soon [182]. Also, the effect on viral RNA levels upon non-adherence of LA ARV nanoformulation also remains to be established in near future.

7. Conclusion

The successful preclinical and clinical leads of two potential LA ARV nanoformulations namely; cabotegravir and rilpivirine with higher potency, half-life, sustained plasma and tissue-specific depot and established regulatory approval for each was indeed a presentation of the new application for older antiretrovirals. Since then, efforts have been made to either synthesize long-acting chemical moieties and their transition into LA nanoformulations. Advent of LA nanoformulations in the future will replace the currently available complex oral cART with a simplified regimen. Various nanocarriers, including solid drug nanocarriers, polymeric nanoparticles, nanosuspension, solid drug nanoparticles, and rod-shaped nanocarriers, could be utilized as platform technology to deliver combination antiretroviral drugs for long term with the creation of cell and tissue-specific secondary depot. However, the physicochemical properties and stability of nanocarriers needs to be thoroughly investigated. Despite of increased preclinical adherence, efficacy and safety, the effect of long-term dosing, tissue pharmacokinetics and its correlation with plasma time profile should be visited for LA nanoformulations to enter into the clinical phase. Moreover, proper selection of viral strain and *in vivo* species is essential to extrapolate the findings onto humans. With an increasing fascination for LA nanoformulation, the effect of non-adherence or switch to oral cART on viral load, drug resistance, and induction from latency after a year or two need to be established. Further, the role of drug metabolism and drug transporters at the injection site should also be elucidated during the development of LA nanoformulation., Surpassing few drawbacks, LA nanoformulations can maintain effective concentration at HIV infection site, spread site, and residence site in great capacities.

Acknowledgements

Dhanashree H. Surve would like to acknowledge Birla Institute of Technology and Science, Pilani-campus, Pilani for providing fellowship and immeasurable support.

References

[1] Antiretroviral Drug Discovery and Development, (2020), pp. 3–5 https://www.niaid.nih.gov/diseases-conditions/antiretroviral-drug-development , Accessed date: 17 April 2020.
[2] UNAIDS, Global HIV & AIDS statistics — 2019 fact sheet, (2020).
[3] HIV/AIDS, https://www.who.int/news-room/fact-sheets/detail/hiv-aids, (2019) , Accessed date: 17 April 2020.
[4] R. Anokye, E. Acheampong, A. Budu-ainooson, E.I. Obeng, E. Tetteh, Y.S. Acheampong, C.E. Nettey-marbell, Knowledge of HIV/AIDS among older adults (50 years and above) in a peri-urban setting: a descriptive cross-sectional study, BMC Geriatr. 19 (2019) 1–8.
[5] J.B. Nachega, V.C. Marconi, G.U. Van Zyl, E.M. Gardner, W. Preiser, S.Y. Hong, E.J. Mills, R. Gross, C. Town, S. Africa, HIV treatment adherence, drug resistance, virologic failure: evolving concepts, Infect Disord Drug Targets 11 (2011) 167–174.
[6] M. Roser, R. Hannah, HIV/AIDS, https://ourworldindata.org/hiv-aids, (2019) , Accessed date: 17 April 2020.
[7] C. Flexner, D.L. Thomas, S. Swindells, Creating demand for long-acting formulations for the treatment and prevention of HIV, tuberculosis, and viral hepatitis, Curr. Opin. HIV AIDS 14 (2019) 13–20, https://doi.org/10.1097/COH.0000000000000510.
[8] D. Sidebottom, A.M. Ekström, S. Strömdahl, A systematic review of adherence to oral pre-exposure prophylaxis for HIV – how can we improve uptake and adherence ? BMC Infect. Dis. 18 (2018) 1–14.
[9] M.B. Hickey, E. Merisko-liversidge, J.F. Remenar, Delivery of long-acting injectable antivirals: best approaches and recent advances, Curr. Opin. Infect. Dis. 28 (2015) 603–610, https://doi.org/10.1097/QCO.0000000000000214.
[10] N.L. Trevaskis, L.M. Kaminskas, C.J.H. Porter, From sewer to saviour — targeting the lymphatic system to promote drug exposure and activity, Nat. Publ. Gr. 14 (2015) 781–803, https://doi.org/10.1038/nrd4608.
[11] T. Zhou, H. Su, P. Dash, Z. Lin, B. Laxmi, D. Shetty, T. Kocher, A. Szlachetka, B. Lamberty, H.S. Fox, L. Poluektova, S. Gorantla, J. Mcmillan, N. Gautam, R.L. Mosley, Y. Alnouti, B. Edagwa, H.E. Gendelman, Creation of a nanoformulated cabotegravir prodrug with improved antiretroviral profiles, Biomaterials. 151 (2018) 53–65, https://doi.org/10.1016/j.biomaterials.2017.10.023.
[12] J. Kraft, L. McConnachie, J. Koehn, L. Kinman, J. Sun, A. Collier, C. Collins, D. Shen, R. Ho, Mechanism-based pharmacokinetic (MBPK) models describe the complex plasma kinetics of three antiretrovirals delivered by a long-acting anti-HIV drug combination nanoparticle formulation, J. Control. Release 275 (2018) 229–241, https://doi.org/10.1016/j.jconrel.2018.02.003.
[13] W.R. Spreen, D.A. Margolis, J.C. Pottage, Long-acting injectable antiretrovirals for HIV treatment and prevention, Curr. Opin. HIV AIDS 8 (2013) 565–571, https://doi.org/10.1097/COH.0000000000000002.
[14] L. Tatham, S. Rannard, A. Owen, Nanoformulation strategies for the enhanced oral bioavailability of antiretroviral therapeutics, Ther. Deliv. 6 (2015) 469–490.
[15] M. Barnhart, Long-acting tretament and prevention: closer to the threshold, Glob. Heal. Sci. Pract. 5 (2017) 182–187.
[16] H.E. Gendelman, J. Mcmillan, A.N. Bade, B. Edagwa, B.D. Kevadiya, The promise of long-acting antiretroviral therapies: from need to manufacture, Trends Microbiol. 27 (2019) 593–606, https://doi.org/10.1016/j.tim.2019.02.009.
[17] A. Owen, S. Rannard, Strengths, weaknesses, opportunities and challenges for long acting injectable therapies: insights for applications in HIV therapy, Adv. Drug Deliv. Rev. 103 (2016) 144–156, https://doi.org/10.1016/j.addr.2016.02.003.
[18] H.M. Jones, R.K. Yeo, Basic Concepts in Physiologically Based Pharmacokinetic Modeling in Drug Discovery and Development, CPT Pharmacometrics Syst. Pharmacol. 2 (2013) 1–12, https://doi.org/10.1038/psp.2013.41.
[19] F. Khalil, L. Stephanie, Physiologically based pharmacokinetic modeling: methodology, applications, and limitations with a focus on its role in pediatric drug development, J. Biomed. Biotechnol. 2011 (2011) 1–13, https://doi.org/10.1155/2011/907461.
[20] B. Ploeger, P. Graaf, M. Danhof, Incorporating receptor theory in mechanism-based pharmacokinetic-pharmacodynamic (PK-PD) modeling, Drug Metab. Pharmacokinet. 24 (2009) 3–15, https://doi.org/10.2133/dmpk.24.3.
[21] M. Danhof, J. Dejongh, E. De Lange, Mechanism-based pharmacokinetic-pharmacodynamic modeling: biophase mechanism-based pharmacokinetic-pharmacodynamic modeling: biophase distribution, receptor theory, and dynamical systems analysis, Annu. Rev. Pharmacol. Toxicol. 47 (2007) 21.1–21.44, https://doi.org/10.1146/annurev.pharmtox.47.120505.105154.
[22] C.C. Nixon, M. Mavigner, G. Silvestri, J.V. Garcia, In vivo models of human immunodeficiency virus persistence and cure strategies, J. Infect. Dis. 215 (2017)

142–151, https://doi.org/10.1093/infdis/jiw637.
[23] B. Sharma, Exploring experimental animal models in HIV / AIDS research, Biochem. Anal. Biochem. 2 (2013) 2–4, https://doi.org/10.4172/2161-1009.1000129.
[24] P. Denton, V.J. Garcia, Humanized mouse models of HIV infection, AIDS Rev. 13 (2011) 135–148.
[25] J.K. Skelton, A.M. Ortega-prieto, A Hitchhiker ' s guide to humanized mice: new pathways to studying viral infections, Immunology. 154 (2018) 50–61, https://doi.org/10.1111/imm.12906.
[26] J.B. Honeycutt, A. Wahl, N. Archin, S. Choudhary, D. Margolis, J.V. Garcia, HIV-1 infection, response to treatment and establishment of viral latency in a novel humanized T cell-only mouse (TOM) model, Retrovirology. 10 (2013) 1–12, https://doi.org/10.1186/1742-4690-10-121.
[27] Y. Gao, J.C. Kraft, D. Yu, R.J.Y. Ho, Recent developments of nanotherapeutics for targeted and long- acting, combination HIV chemotherapy, Eur. J. Pharm. Biopharm. 138 (2019) 75–91, https://doi.org/10.1016/j.ejpb.2018.04.014.Recent.
[28] Prescribing Information for Genvoya, (2016), pp. 1–50 https://www.accessdata.fda.gov/drugsatfda_docs/label/2016/207561s002lbl.pdf , Accessed date: 13 May 2020.
[29] Stribild 150 mg/150 mg/200 mg/245 mg Film-Coated Tablets, https://www.medicines.org.uk/emc/product/3154/smpc, (2020) , Accessed date: 13 May 2020.
[30] Prescribing Information for Symtuza, http://www.janssenlabels.com/package-insert/product-monograph/prescribing-information/SYMTUZA-pi.pdf, (2020) , Accessed date: 13 May 2020.
[31] Summary of Product Characteristics, (2020), pp. 1–38 https://www.ema.europa.eu/en/documents/product-information/biktarvy-epar-product-information_en.pdf , Accessed date: 13 May 2020.
[32] Y. Gao, J.C. Kraft, D. Yu, R.J.Y. Ho, Recent developments of nanotherapeutics for targeted and long-acting, combination HIV chemotherapy, Eur. J. Pharm. Biopharm. (2018), https://doi.org/10.1016/j.ejpb.2018.04.014.
[33] Efavirenz / Emtricitabine / Tenofovir Disoproxil Fumarate, https://aidsinfo.nih.gov/drugs/424/atripla/0/patient, (2020) , Accessed date: 13 May 2020.
[34] Emtricitabine / Rilpivirine / Tenofovir Disoproxil Fumarate, https://aidsinfo.nih.gov/drugs/441/complera/5/professional, (2020) , Accessed date: 13 May 2020.
[35] Delstrigo Summary of Product Characteristics, https://www.ema.europa.eu/en/documents/product-information/delstrigo-epar-product-information_en.pdf, (2020) , Accessed date: 13 May 2020.
[36] Doravirine, https://pubchem.ncbi.nlm.nih.gov/compound/Doravirine, (2020) , Accessed date: 13 May 2020.
[37] Emtricitabine/Rilpivirine/Tenofovir AF (Rx), https://reference.medscape.com/drug/odefsey-emtricitabine-rilpivirine-tenofovir-af-1000079, (2020) , Accessed date: 13 May 2020.
[38] Efavirenz, Lamivudine and Tenofovir Disoproxil Fumarate Tablets, Lamivudine and Tenofovir Disoproxil Fumarate Tablets.html, http://www.druginformation.com/RxDrugs/E/Efavirenz, (2020) , Accessed date: 13 May 2020.
[39] Prescribing Information for Triumeq, https://www.accessdata.fda.gov/drugsatfda_docs/label/2014/205551s000lbl.pdf, (2014) , Accessed date: 13 May 2020.
[40] Trizivir 300 mg/150 mg/300 mg Film-Coated Tablets, https://www.medicines.org.uk/emc/product/1307/smpc, (2020) , Accessed date: 13 May 2020.
[41] Prescribing Information for JULUCA, https://www.gsksource.com/pharma/content/dam/GlaxoSmithKline/US/en/Prescribing_Information/Juluca/pdf/JULUCA-PI-PIL.PDF, (2019).
[42] Lamivudine/Zidovudine, https://aidsinfo.nih.gov/drugs/285/combivir/164/professional, (2020) , Accessed date: 13 May 2020.
[43] Prescribing Information for Descovy, https://www.gilead.com/-/media/files/pdfs/medicines/hiv/descovy/descovy_pi.pdf, (2020) , Accessed date: 13 May 2020.
[44] Abacavir/Lamivudine, https://aidsinfo.nih.gov/drugs/407/epzicom/6/professional, (2020) , Accessed date: 13 May 2020.
[45] Emtricitabine/Tenofovir DF (Rx), https://reference.medscape.com/drug/truvada-emtricitabine-tenofovir-df-342640, (2020) , Accessed date: 13 May 2020.
[46] Atazanavir / Cobicistat, https://aidsinfo.nih.gov/drugs/537/evotaz/175/professional, (2020) , Accessed date: 13 May 2020.
[47] Kaletra 200 mg/50 mg Film-Coated Tablets, https://www.medicines.org.uk/emc/product/221, (2020) , Accessed date: 13 May 2020.
[48] Kaletra Dosage, https://www.drugs.com/dosage/kaletra.html, (2020) , Accessed date: 13 May 2020.
[49] PREZCOBIX® (Darunavir And Cobicistat) Tablets, https://www.rxlist.com/prezcobix-drug.htm, (2020) , Accessed date: 13 May 2020.
[50] J.R. Hilaire, A.N. Bade, B. Sillman, N. Gautam, J. Herskovitz, B. Laxmi, D. Shetty, M.S. Wojtkiewicz, A. Szlachetka, B.G. Lamberty, S. Sravanam, H.S. Fox, Y. Alnouti, P.K. Dash, J.M. Mcmillan, B.J. Edagwa, H.E. Gendelman, Creation of a long-acting rilpivirine prodrug nanoformulation, J. Control. Release 311–312 (2019) 201–211, https://doi.org/10.1016/j.jconrel.2019.09.001.
[51] P. Puligujja, S.S. Balkundi, L.M. Kendrick, H.M. Baldridge, J.R. Hilaire, A.N. Bade, P.K. Dash, G. Zhang, L.Y. Poluektova, S. Gorantla, X. Liu, T. Ying, Y. Feng, Y. Wang, D.S. Dimitrov, J.M. Mcmillan, H.E. Gendelman, Pharmacodynamics of long-acting folic acid-receptor targeted ritonavir-boosted atazanavir nanoformulations, Biomaterials. 41 (2015) 141–150, https://doi.org/10.1016/j.biomaterials.2014.11.012.
[52] S. Mandal, P.K. Prathipati, G. Kang, Y. Zhao, Z. Yuan, W. Fan, Q. Li, C. Destache, Tenofovir alafenamide and elvitegravir loaded nanoparticles for long-acting prevention of HIV-1 vaginal transmission, AIDS. 31 (2018) 469–476, https://doi.org/10.1097/QAD.0000000000001349.Tenofovir.
[53] S. Mandal, G. Kang, P. Kumar, Y. Zhou, W. Fan, Q. Li, C.J. Destache, Nanoencapsulation introduces long-acting phenomenon to tenofovir alafenamide and emtricitabine drug combination: a comparative pre- exposure prophylaxis e ffi cacy study against HIV-1 vaginal transmission, J. Control. Release 294 (2019) 216–225, https://doi.org/10.1016/j.jconrel.2018.12.027.
[54] Z. Lin, N. Gautam, Y. Alnouti, J. Mcmillan, A.N. Bade, H.E. Gendelman, B. Edagwa, ProTide generated long-acting abacavir nanoformulations, Chem. Commun. 54 (2018) 8371–8374, https://doi.org/10.1039/c8cc04708a.
[55] J.M. Jacobson, C. Flexner, I. Diseases, Universal Antiretroviral Regimens: Thinking Beyond One-Pill- Once-a-Day, Curr. Opin. HIV AIDS 12 (2017) 343–350, https://doi.org/10.1097/COH.0000000000000374.Universal.
[56] S. Swindells, M. Siccardi, S.E. Barrett, D.B. Olsen, J.A. Grobler, A. Podany, E. Nuermberger, P. Kim, C. Barry, A. Owen, Long-acting formulations for the treatment of latent Tuberculosis infection: Opportunities and Challenges, Int J Tuberc Lung Dis. 22 (2018) 125–132, https://doi.org/10.5588/ijtld.17.0486.LONG-ACTING.
[57] Q. Mu, J. Yu, L.A. Mcconnachie, J.C. Kraft, Y. Gao, G.K. Gulati, R.J.Y. Ho, Translation of combination nanodrugs into nanomedicines: lessons learned and future outlook, J. Drug Target. 26 (2018) 435–447, https://doi.org/10.1080/1061186X.2017.1419363.Translation.
[58] W.R. Spreen, D.A. Margolis, J.C. Pottage, Long-acting injectable antiretrovirals for HIV treatment and prevention, Curr. Opin. HIV AIDS 8 (2013) 565–571, https://doi.org/10.1097/COH.0000000000000002.
[59] C.A. Lipinski, F. Lombardo, B. Dominy, P. Feeney, Experimental and computational approaches to estimate solubility and permeability in drug discovery and development settings, Adv. Drug Deliv. Rev. 23 (1997) 3–25.
[60] T. Oashi, A. Ringer, P. Raman, A.D. MacKrell, Automated selection of compounds with physicochemical properties to maximize bioavailability and druglikeness, J. Chem. Inf. Model. 51 (2012) 148–158, https://doi.org/10.1021/ci100359a.Automated.
[61] B.C. Doak, F. Giordanetto, J. Kihlberg, Oral druggable space beyond the rule of 5: insights from drugs and clinical candidates, Chem. Biol. 21 (2014) 1115–1142, https://doi.org/10.1016/j.chembiol.2014.08.013.
[62] J.F. Remenar, Making the leap from daily oral dosing to long-acting injectables: lessons from the antipsychotics, Mol. Pharm. 11 (2014) 1739–1749.
[63] I.M. Ibrahim, D. Soni, H.E. Gendelman, Synthesis and characterization of a long-acting emtricitabine prodrug nanoformulation, Int. J. Nanomedicine 14 (2019) 6231–6247.
[64] N. Smith, A.N. Bade, D. Soni, N. Gautam, Y. Alnouti, J. Herskovitz, I.M. Ibrahim, M.S. Wojtkiewicz, B. Laxmi, D. Shetty, J. Mcmillan, H.E. Gendelman, B. Edagwa, A long acting nanoformulated lamivudine ProTide, Biomaterials. 223 (2019) 1–11, https://doi.org/10.1016/j.biomaterials.2019.119476.
[65] J. Duan, J.P. Freeling, J. Koehn, C. Shu, R.J.Y. Ho, Evaluation of atazanavir and darunavir interactions with lipids for developing pH-responsive anti-HIV drug combination nanoparticles, J. Pharm. Sci. 103 (2014) 2520–2529, https://doi.org/10.1002/jps.24046.Evaluation.
[66] G.V.J. Klooster, E. Hoeben, H. Borghys, A. Looszova, M. Bouche, F. Van Velsen, L. Baert, Pharmacokinetics and disposition of rilpivirine (TMC278) nanosuspension as a long-acting injectable antiretroviral formulation, Antimicrob. Agents Chemother. 54 (2010) 2042–2050, https://doi.org/10.1128/AAC.01529-09.
[67] K. Palm, P. Stenberg, K. Luthman, P. Artursson, Polar molecular surface properties predict the intestinal absorption of drugs in humans, Pharm. Res. 14 (1997) 568–571.
[68] L.Z. Benet, F. Broccatelli, T.I. Oprea, BDDCS applied to over 900 drugs, AAPS J. 13 (2011) 519–546, https://doi.org/10.1208/s12248-011-9290-9.
[69] L.Z. Benet, C.M. Hosey, O. Ursu, T.I. Oprea, BDDCS, the rule of 5 and drugability, Adv. Drug Deliv. Rev. 101 (2016) 89–98, https://doi.org/10.1016/j.addr.2016.05.007.BDDCS.
[70] C.M.O. Driscoll, B.T. Griffin, Biopharmaceutical challenges associated with drugs with low aqueous solubility — The potential impact of lipid-based formulations ☆, Adv. Drug Deliv. Rev. 60 (2008) 617–624, https://doi.org/10.1016/j.addr.2007.10.012.
[71] M.R. Gigliobianco, C. Casadidio, R. Censi, P. Di MArtino, Nanocrystals of poorly soluble drugs: drug bioavailability and physicochemical stability, Pharmaceutics. 10 (2018) 1–29, https://doi.org/10.3390/pharmaceutics10030134.
[72] A.R. Kirtane, O. Abouzid, D. Minahan, T. Bensel, A.L. Hill, C. Selinger, A. Bershteyn, M. Craig, S.S. Mo, H. Mazdiyasni, C. Cleveland, J. Rogner, Y.L. Lee, L. Booth, F. Javid, S.J. Wu, T. Grant, A.M. Bellinger, B. Nikolic, A. Hayward, L. Wood, P.A. Eckhoff, M.A. Nowak, R. Langer, G. Traverso, Development of an oral once-weekly drug delivery system for HIV antiretroviral therapy, Nat. Commun. 9 (2018) 1–12, https://doi.org/10.1038/s41467-017-02294-6.
[73] T. Zhou, H. Su, P. Dash, Z. Lin, B. Laxmi, D. Shetty, T. Kocher, A. Szlachetka, B. Lamberty, H.S. Fox, L. Poluektova, S. Gorantla, J. Mcmillan, N. Gautam, R.L. Mosley, Y. Alnouti, B. Edagwa, H.E. Gendelman, Creation of a nanoformulated cabotegravir prodrug with improved antiretroviral profiles, Biomaterials 151 (2018) 53–65, https://doi.org/10.1016/j.biomaterials.2017.10.023.
[74] S.A. Hassounah, T. Mesplède, Where are we with injectables against HIV infection and what are the remaining challenges? Expert Rev. Anti-Infect. Ther. 16 (2018) 143–152, https://doi.org/10.1080/14787210.2018.1430570.
[75] E. Ahire, S. Thakkar, M. Darshanwad, M. Misra, Parenteral nanosuspensions: a brief review from solubility enhancement to more novel and speci fi c applications, Acta Pharm. Sin. B 8 (2018) 733–755, https://doi.org/10.1016/j.apsb.2018.07.011.
[76] L. Baert, G. Van, W. Dries, M. François, A. Wouters, E. Basstanie, K. Iterbeke, F. Stappers, P. Stevens, L. Schueller, P. Van Remoortere, G. Kraus, P. Wigerinck, J. Rosier, Development of a long-acting injectable formulation with nanoparticles

of rilpivirine (TMC278) for HIV treatment, Eur. J. Pharm. Biopharm. 72 (2009) 502–508, https://doi.org/10.1016/j.ejpb.2009.03.006.
[77] R.J. Landovitz, S. Li, B.G. Id, H. Dawood, A.Y. Liu, M. Magnus, M.C. Hosseinipour, R. Panchia, L. Cottle, G. Chau, P. Richardson, M.A. Marzinke, C.W. Hendrix, S. Eshleman, Y. Zhang, T. Elizabeth, J. Sugarman, R. Kofron, A. Adeyeye, D. Burns, A.R. Rinehart, D. Margolis, W.R. Spreen, M.S. Cohen, M. Mccauley, J.J.E. Id, Safety, tolerability, and pharmacokinetics of long-acting injectable cabotegravir in low-risk HIV-uninfected individuals: HPTN 077, a phase 2a randomized controlled trial, PLOS Med. Med. 15 (2018) 1–22.
[78] J. Scallan, V. Huxley, R. Korthuis, The Lymphatic Vasculature, in: Capill, Fluid Exch. Regul. Funct. Pathol. (2010).
[79] A.A. Khan, J. Mudassir, N. Mohtar, Y. Darwis, Advanced drug delivery to the lymphatic system: lipid-based nanoformulations, Int. J. Nanomedicine 8 (2013) 2733–2744.
[80] J.E. Moore, C.D. Bertram, Lymphatic system flows, Annu. Rev. Fluid Mech. 50 (2018) 459–482, https://doi.org/10.1146/annurev-fluid-122316-045259. Lymphatic.
[81] M. Horiike, S. Iwami, M. Kodama, A. Sato, Y. Watanabe, M. Yasui, Lymph nodes harbor viral reservoirs that cause rebound of plasma viremia in SIV-infected macaques upon cessation of combined antiretroviral therapy, Virology. 423 (2012) 107–118, https://doi.org/10.1016/j.virol.2011.11.024.
[82] Y. Dimopoulos, E. Moysi, C. Petrovas, The Lymph Node in HIV Pathogenesis, Curr HIV/AIDS Rep, (2017), https://doi.org/10.1007/s11904-017-0359-7.
[83] A.R. Abell, M.J.S. Erea, B. Anxo, V. Marcos, Polyaminoacid nanocapsules for drug delivery to the lymphatic system: effect of the particle size, Int. J. Pharm. 509 (2016) 107–117, https://doi.org/10.1016/j.ijpharm.2016.05.034.
[84] S. Aquaro, R. Calio, J. Balzarini, C. Bellocchi, E. Garaci, C. Federico, Macrophages and HIV infection: therapeutical approaches toward this strategic virus reservoir, Antivir. Res. 55 (2002) 209–225.
[85] V. Schafer, H. von Briesen, R. Andreesen, A.-M. Steffan, C. Royer, S. Troster, J. Kreuter, H.R. Waigmann, Phagocytosis of Nanoparticles by Human Immunodeficiency Virus (HIV)-Infected Macrophages: A Possibility for Antiviral Drug Targeting, Pharm. Res. 9 (1992) 541–546.
[86] S.X. Jin, D.Z. Bi, J. Wang, Y.Z. Wang, H.G. Hu, Y.H. Deng, Pharmacokinetics and tissue distribution of zidovudine in rats following intravenous administration of zidovudine myristate loaded liposomes, Pharmazie. 60 (2005) 99–102.
[87] H. Dou, C.B. Grotepas, J.M. Mcmillan, C.J. Destache, J. Werling, J. Kipp, B. Rabinow, H.E. Gendelman, Macrophage delivery of nanoformulated antiretroviral drug to the brain in a murine model of neuroAIDS, J. Immunol. 183 (2009) 661–669, https://doi.org/10.4049/jimmunol.0900274.Macrophage.
[88] A.L. Martinez-skinner, M.A. Araínga, P. Puligujja, D.L. Palandri, Cellular Responses and Tissue Depots for Nanoformulated Antiretroviral Therapy, PLoS One 10 (2015) 1–19, https://doi.org/10.1371/journal.pone.0145966.
[89] N. Gautam, U. Roy, S. Balkundi, P. Puligujja, D. Guo, N. Smith, X. Liu, Preclinical Pharmacokinetics and Tissue Distribution of Long-Acting Nanoformulated Antiretroviral Therapy, Antimicrob. Agents Chemother. 57 (2013) 3110–3120, https://doi.org/10.1128/AAC.00267-13.
[90] L.M. Tatham, A.C. Savage, A. Dwyer, M. Siccardi, T. Scott, M. Vourvahis, A. Clark, S.P. Rannard, A. Owen, Towards a Maraviroc long-acting injectable nanoformulation, Eur. J. Pharm. Biopharm. (2018), https://doi.org/10.1016/j.ejpb.2018.04.009.
[91] S. Perazzolo, L.M. Shireman, L.A. Mcconnachie, J.C. Kraft, D.D. Shen, R.J.Y. Ho, Three HIV drugs, atazanavir, ritonavir, and tenofovir, coformulated in drug-combination nanoparticles exhibit long-acting and lymphocyte-targeting properties in nonhuman primates, J. Pharm. Sci. 101 (2018) 1–10, https://doi.org/10.1016/j.xphs.2018.07.032.
[92] J. Freeling, J. Koehn, C. Shu, J. Sun, R. Ho, Anti-HIV drug-combination nanoparticles enhance as well as triple-drug combination levels in cells within lymph nodes and blood in primates, AIDS Res. Hum. Retrviruses. 31 (2015) 107–114, https://doi.org/10.1089/aid.2014.0210.
[93] J. Freeling, J. Koehn, C. Shu, J. Sun, R. Ho, Long-acting three-drug combination anti-HIV nanoparticles enhance drug exposure in primate plasma and cells within lymph nodes and blood, AIDS. 28 (2014) 2625–2631.
[94] S.N. Kudalkar, I. Ullah, N. Bertoletti, H.K. Mandl, J.A. Cisneros, J. Beloor, A.H. Chan, E. Quijano, W.M. Saltzman, W.L. Jorgensen, P. Kumar, K.S. Anderson, Structural and pharmacological evaluation of a novel non-nucleoside reverse transcriptase inhibitor as a promising long acting nanoformulation for treating HIV, Antivir. Res. 167 (2019) 110–116, https://doi.org/10.1016/j.antiviral.2019.04.010.
[95] S. Mandal, G. Kang, P. Kumar, W. Fan, Q. Li, C.J. Destache, Long-acting parenteral combination antiretroviral loaded nano-drug delivery system to treat chronic HIV-1 infection: A humanized mouse model study, Antivir. Res. 156 (2018) 85–91, https://doi.org/10.1016/j.antiviral.2018.06.005.
[96] C. Trezza, S.L. Ford, W. Spreen, R. Pan, Formulation and pharmacology of long-acting cabotegravir, Curr. Opin. HIV AIDS 10 (2015) 239–245, https://doi.org/10.1097/COH.0000000000000168.
[97] P.E. Williams, H.M. Crauwels, E.D. Basstanie, Formulation and pharmacology of long-acting rilpivirine, Curr. Opin. HIV AIDS 10 (2015) 233–238, https://doi.org/10.1097/COH.0000000000000164.
[98] Y. Lu, Y. Li, W. Wu, Injected nanocrystals for targeted drug delivery, Acta Pharm. Sin. B 6 (2016) 106–113, https://doi.org/10.1016/j.apsb.2015.11.005.
[99] M.K. Rainer, Risperidone long-acting injection: a review of its long term safety and ef fi cacy, Neuropsychiatr. Dis. Treat. 4 (2008) 919–927.
[100] P. Chue, J. Chue, A critical appraisal of paliperidone long-acting injection in the treatment of schizoaffective disorder, Ther. Clin. Risk Manag. 12 (2016) 109–116.
[101] J. Lindenmayer, Long-acting injectable antipsychotics: focus on olanzapine pamoate, Neurol. Res. 6 (2010) 261–267.
[102] M. Monroe, C. Flexner, H. Cui, Harnessing nanostructured systems for improved treatment and prevention of HIV disease, Bioeng. Transl. Med. 3 (2018) 102–123, https://doi.org/10.1002/btm2.10096.
[103] K. Singh, S.G. Sarafianos, A. Sönnerborg, Long-Acting Anti-HIV Drugs Targeting HIV-1 Reverse Transcriptase and Integrase, Pharmaceuticals. 12 (2019) 1–14.
[104] G.D. Bowers, A. Culp, M.J. Reese, G. Tabolt, L. Moss, S. Piscitelli, P. Huynh, D. Wagner, S.L. Ford, P. Elizabeth, R. Pan, Y. Lou, D.A. Margolis, W.R. Spreen, G. David, A. Culp, M.J. Reese, G. Tabolt, S. Piscitelli, P. Huynh, D. Wagner, S.L. Ford, E.P. Gould, R. Pan, Y. Lou, D.A. Margolis, W.R.S. Disposition, P. Huynh, D. Wagner, S.L. Ford, E.P. Gould, R. Pan, Y. Lou, D.A. Margolis, Disposition and metabolism of cabotegravir: a comparison of biotransformation and excretion between different species and routes of administration in humans Disposition and metabolism of cabotegravir: a comparison of biotransformation and excretion betw, Xenobiotica (2015) 1–16, https://doi.org/10.3109/00498254.2015.1060372.
[105] B.M. Jucker, H. Alsaid, M. Rambo, S.C. Lenhard, B. Hoang, F. Xie, M.R. Groseclose, S. Castellino, V. Damian, G. Bowers, M. Gupta, Multimodal imaging approach to examine biodistribution kinetics of Cabotegravir (GSK1265744) long acting parenteral formulation in rat, J. Control. Release 268 (2017) 102–112, https://doi.org/10.1016/j.jconrel.2017.10.017.
[106] D. Cattaneo, C. Gervasoni, Pharmacokinetics and pharmacodynamics of cabotegravir, a long - acting hiv integrase strand transfer inhibitor, Eur. J. Drug Metab. Pharmacokinet. (2018), https://doi.org/10.1007/s13318-018-0526-2.
[107] C.D. Andrews, L.S.T. Bernard, A.Y. Poon, H. Mohri, W.R. Spreen, A. Gettie, K. Russell-lodrigue, J. Blanchard, Z. Hong, D.D. Ho, M. Markowitz, Cabotegravir long-acting injection protects macaques against intravenous challenge with SIVmac251, AIDS. 31 (2017) 461–467, https://doi.org/10.1097/QAD.0000000000001343.Cabotegravir.
[108] C.D. Andrews, Y.L. Yueh, W.R. Spreen, L.S. Bernard, M. Boente, K. Rodriguez, A. Gettie, K. Russell-lodrigue, S. Ford, H. Mohri, C. Cheng-mayer, Z. Hong, D.D. Ho, M. Markowitz, A long-acting integrase inhibitor protects female macaques from repeated high-dose intravaginal SHIV challenge, Sci. Transl. Med. 7 (2015), https://doi.org/10.1126/scitranslmed.3010298.A.
[109] ViiV Healthcare Submits New Drug Application to US FDA for the First Monthly, Injectable, Two-Drug Regimen of Cabotegravir and Rilpivirine for Treatment of HIV, https://www.gsk.com/en-gb/media/press-releases/viiv-healthcare-submits-new-drug-application-to-us-fda-for-the-first-monthly-injectable-two-drug-regimen-of-cabotegravir-and-rilpivirine-for-treatment-of-hiv/, (2019) , Accessed date: 25 April 2020.
[110] Janssen Announces Health Canada Approval of CABENUVA™, the First Long-Acting Regimen for the Treatment of HIV, https://www.jnj.com/janssen-announces-health-canada-approval-of-cabenuva-the-first-long-acting-regimen-for-the-treatment-of-hiv, (2020) , Accessed date: 11 May 2020.
[111] S. Moreno, C.F. Perno, P.W. Mallon, G. Behrens, P. Corbeau, J. Routy, G. Darcis, Two-drug vs. three-drug combinations for HIV-1: do we have enough data to make the switch ? HIV Med. 20 (2019) 2–12, https://doi.org/10.1111/hiv.12716.
[112] HPTN, 076 Phase II Safety and Acceptability of an Investigational Injectable Product, TMC278 LA, for Pre Exposure Prophylaxis (PrEP), https://www.hptn.org/research/studies/hptn076, (2017) , Accessed date: 24 April 2020.
[113] T. Hptn, E.E. Tolley, S. Li, S.Z. Zangeneh, M. Atujuna, P. Musara, J. Justman, S. Pathak, L. Bekker, S. Swaminathan, J. Stanton, J. Farrior, N. Sista, Acceptability of a long-acting injectable HIV prevention product among US and African women: findings from a phase 2 clinical Trial (HPTN 076), J. Int. AIDS Soc. 22 (2019) 1–9, https://doi.org/10.1002/jia2.25408/full.
[114] A. Safety, Tolerability, Acceptability, and Pharmacokinetic (PK) Study of Cabotegravir (CAB) in Healthy Human Immunodeficiency Virus (HIV)-Uninfected Chinese Men, https://clinicaltrials.gov/ct2/show/NCT03422172, (2020) , Accessed date: 24 April 2020.
[115] M. Markowitz, I. Frank, R.M. Grant, K.H. Mayer, R. Elion, D. Goldstein, C. Fisher, M.E. Sobieszczyk, A.R. Rinehart, K.Y. Smith, W.R. Spreen, Safety and tolerability of long-acting cabotegravir injections in HIV-uninfected men (ECLAIR): a multicentre, double-blind, randomised, placebo-controlled, phase 2a trial, Lancet HIV. (2017) 1–10, https://doi.org/10.1016/S2352-3018(17)30068-1.
[116] Safety and Efficacy Study of Injectable Cabotegravir Compared to Daily Oral Tenofovir Disoproxil Fumarate/Emtricitabine (TDF/FTC), For Pre-Exposure Prophylaxis in HIV-Uninfected Cisgender Men and Transgender Women Who Have Sex With Men, https://clinicaltrials.gov/ct2/show/NCT02720094, (2020) , Accessed date: 24 April 2020.
[117] R. Verloes, S. Deleu, N. Niemeijer, H. Crauwels, P. Meyvisch, P. Williams, Safety, tolerability and pharmacokinetics of rilpivirine following administration of a long-acting formulation in healthy volunteers *, HIV Med. 16 (2015) 477–484, https://doi.org/10.1111/hiv.12247.
[118] I. Mcgowan, C.S. Dezzutti, A. Siegel, J. Engstrom, A. Nikiforov, K. Duffi, C. Shetler, N. Richardson-harman, K. Abebe, D. Back, L. Else, D. Egan, S. Khoo, J.E. Egan, R. Stall, P.E. Williams, K.K. Rehman, A. Adler, R.M. Brand, B. Chen, S. Achilles, R.D. Cranston, F. Bill, M.G. Foundation, Long-acting rilpivirine as potential pre-exposure prophylaxis for HIV-1 prevention (the MWRI-01 study): an open-label, phase 1, compartmental, pharmacokinetic and pharmacodynamic assessment, Lancet HIV 3018 (2016) 1–10, https://doi.org/10.1016/S2352-3018(16)30113-8.
[119] W. Spreen, S.L. Ford, S. Chen, D. Wilfret, D. Margolis, E. Gould, S. Piscitelli, GSK1265744 pharmacokinetics in plasma and tissue after single-dose long-acting injectable administration in healthy subjects, J. Acquir. Immune Defic. Syndr. 67 (2014) 481–486.
[120] Pharmacokinetic Study of Cabotegravir Long-acting in Healthy Adult Volunteers, https://clinicaltrials.gov/ct2/show/NCT02478463, (2020) , Accessed date: 24

April 2020.
[121] R. Parasrampuria, S.L. Ford, Y. Lou, C. Fu, K.K. Bakshi, A.R. Tenorio, C. Trezza, W.R. Spreen, P. Patel, A phase i study to evaluate the pharmacokinetics and safety of cabotegravir in adults with severe renal impairment and healthy, Clin. Pharmacol. Drug Dev. 8 (2019) 674–681, https://doi.org/10.1002/cpdd.664.
[122] Long-Acting Cabotegravir Plus VRC-HIVMAB075-00-AB (VRC07-523LS) for Viral Suppression in Adults Living With HIV-1, https://clinicaltrials.gov/ct2/show/NCT03739996, (2020) , Accessed date: 24 April 2020.
[123] Phase 2b, Open-label, Multicenter, Rollover Study to Assess Antiviral Activity and Safety of Long-acting Cabotegravir (CAB LA) Plus Long-acting Rilpivirine (RPV LA), Administered Every 2 Months (Q2M), in Human Immunodeficiency Virus (HIV)- Positive Subjec, https://clinicaltrials.gov/ct2/show/NCT03639311, (2020) , Accessed date: 24 April 2020.
[124] D.A. Margolis, J. Gonzalez-garcia, H. Stellbrink, J.J. Eron, Y. Yazdanpanah, D. Podzamczer, T. Lutz, J.B. Angel, G.J. Richmond, B. Clotet, F. Gutierrez, L. Sloan, M.S. Clair, M. Murray, S.L. Ford, J. Mrus, P. Patel, H. Crauwels, S.K. Griffith, K.C. Sutton, D. Dorey, K.Y. Smith, P.E. Williams, W.R. Spreen, Long-acting intramuscular cabotegravir and rilpivirine in adults with HIV-1 infection (LATTE-2): 96-week results of a randomised, open-label, phase 2b, non-inferiority trial, Lancet 6736 (2017) 1–12, https://doi.org/10.1016/S0140-6736(17)31917-7.
[125] S. Susan, A. Villanueva, G. Richmond, G. Rizzardini, A. Maumgarten, M. Masia, G. Latiff, V. Pokrovsky, J. Mrus, J. Huang, K. Hudson, D. Margolis, K. Smith, P. Williams, S. Williams, Long-acting Cabotegravir + Rilpivirine as maintenance therapy: ATLAS week 48 results, Conf. Retroviruses Opportunistic Infect, 2019.
[126] Study Evaluating the Efficacy, Safety, and Tolerability of Switching to Long-acting Cabotegravir Plus Long-acting Rilpivirine From Current Antiretroviral Regimen in Virologically Suppressed HIV-1-Infected Adults, https://www.clinicaltrials.gov/ct2/show/NCT02951052, (2020) , Accessed date: 24 April 2020.
[127] C. Orkin, K. Arasteh, M.G. Hernández-Mora, V. Pokrovsky, E.T. Overton, P.-M. Girard, S. Oka, R. D'Amico, D. Dorey, S. Griffith, D.A. Margolis, P.E. Williams, W. Parys, W. Spreen, Long-acting Cabotegravir + Rilpivirne for HIV maintenance: FLAIR week 48 results, Conf. Retroviruses Opportunistic Infect, 2019.
[128] Study to Evaluate the Efficacy, Safety, and Tolerability of Long-acting Intramuscular Cabotegravir and Rilpivirine for Maintenance of Virologic Suppression Following Switch From an Integrase Inhibitor in HIV-1 Infected Therapy Naive Participants, https://clinicaltrials.gov/ct2/show/NCT02938520, (2020) , Accessed date: 24 April 2020.
[129] More Options for Children and Adolescents (MOCHA): Oral and Long-Acting Injectable Cabotegravir and Rilpivirine in HIV-Infected Children and Adolescents (MOCHA), https://clinicaltrials.gov/ct2/show/NCT03497676, (2020) , Accessed date: 24 April 2020.
[130] The LATITUDE Study: Long-Acting Therapy to Improve Treatment SUccess in Daily LifE, https://clinicaltrials.gov/ct2/show/NCT03635788, (2020) , Accessed date: 24 April 2020.
[131] B.L. Critchley, How Solid Drug Nanoparticles Can Tackle Drug Adherence Issues, (2018), pp. 4–7 https://www.azonano.com/article.aspx?ArticleID=4974 , Accessed date: 11 April 2020.
[132] S. Onoue, S. Yamada, H. Chan, Nanodrugs: pharmacokinetics and safety, Int. J. Nanomedicine 9 (2014) 1025–1037.
[133] T.O. Mcdonald, M. Giardiello, P. Martin, M. Siccardi, N.J. Liptrott, D. Smith, P. Roberts, P. Curley, A. Schipani, S.H. Khoo, J. Long, A.J. Foster, S.P. Rannard, A. Owen, Antiretroviral solid drug nanoparticles with enhanced oral bioavailability: production, characterization, and in vitro – in vivo correlation, Adv. Heal. Mater. 3 (2014) 400–411, https://doi.org/10.1002/adhm.201300280.
[134] M. Siccardi, P. Martin, D. Smith, P. Curley, T. Mcdonald, M. Giardiello, N. Liptrott, S. Rannard, A. Owen, Towards a rational design of solid drug nanoparticles with optimised pharmacological properties, J. Interdiscip. Nanomed. 1 (2016) 110–123, https://doi.org/10.1002/jin2.21.
[135] A.C. Savage, L.M. Tatham, M. Siccardi, T. Scott, M. Vourvahis, A. Clark, S.P. Rannard, A. Owen, Improving maraviroc oral bioavailability by formation of solid drug nanoparticles, Eur. J. Pharm. Biopharm. 138 (2020) 30–36, https://doi.org/10.1016/j.ejpb.2018.05.015.
[136] H.I.V. London, V. Healthcare, S. Limited, N.D. Application, U.S. Food, ViiV Healthcare Submits New Drug Application to US FDA for the First Monthly, Injectable, Two-Drug Regimen of Cabotegravir and Rilpivirne for Tretament of HIV, https://viivhealthcare.com/en-gb/media/press-releases/2019/april/viiv-healthcare-submits-new-drug-application-to-us-fda-for-the-first-monthly-injectable-two-drug-regimen-of-cabotegravir-and-rilpivirine-for-treatment-of-hiv, (2019) , Accessed date: 11 April 2020.
[137] U. Roy, J. Mcmillan, Y. Alnouti, N. Gautum, N. Smith, S. Balkundi, P. Dash, S. Gorantla, A. Martinez-skinner, J. Meza, G. Kanmogne, S. Swindells, S.M. Cohen, R.L. Mosley, L. Poluektova, H.E. Gendelman, Pharmacodynamic and antiretroviral activities of combination nanoformulated antiretrovirals in HIV-1 – infected human peripheral blood lymphocyte – reconstituted mice, J. Infect. Dis. 206 (2012) 1577–1588, https://doi.org/10.1093/infdis/jis395.
[138] M.G. Banoub, A.N. Bade, Z. Lin, D. Cobb, N. Gautam, B. Laxmi, D. Shetty, M. Wojtkiewicz, Y. Alnouti, J. Mcmillan, H.E. Gendelman, B. Edagwa, Synthesis and characterization of long-acting darunavir prodrugs, Mol. Pharm. 17 (2020) 155–166, https://doi.org/10.1021/acs.molpharmaceut.9b00871.
[139] D. Guo, T. Zhou, M. Araínga, D. Palandri, N. Gautam, T. Bronich, Y. Alnouti, J. Mcmillan, B. Edagwa, H.E. Gendelman, Creation of a long-acting nanoformulated 2',3'-dideoxy-3'-thiacytidine, J. Acquir. Immune Defic. Syndr. 74 (2017) 75–83.
[140] H.E.G. Brady Sillman, Aditya N. Bade, Prasanta K. Dash, Biju Bhargavan, Ted Kocher, Saumi Mathews, Hang Su, Georgette D. Kanmogne, Larisa Y. Pluektova, Santhi Gorantla, JoEllyn McMillan, Nagsen Gautam, Yazen Alnouti, Benson Edagwa, Creation of a long-acting nanoformulated dolutegravir, Nat. Commun. 9 (2018) 1–14, https://doi.org/10.1097/QAI.0000000000001170.
[141] J. Shen, D.J. Burgess, Accelerated in-vitro release testing methods for extended-release parenteral dosage forms, J. Pharm. Pharamcol. 64 (2012) 986–996, https://doi.org/10.1111/j.2042-7158.2012.01482.x.
[142] C. Hansch, J. Bjorkroth, A. Leo, Hydrophobicity and central nervous system agents: On the principle of minimal hydrophobicity in drug deisgn, J. Pharamceutical Sci. 76 (1987) 663–687.
[143] S. Mandal, M. Belshan, A. Holec, Y. Zhou, C. Destache, An enhanced emtricitabine-loaded long-acting nanoformulation for prevention or treatment of hiv infection, Antimicrob. Agents Chemother. 61 (2017) 1–11.
[144] S. Mandal, P. Kumar, M. Belshan, C.J. Destache, A potential long-acting bictegravir loaded nano-drug delivery system for HIV-1 infection: a proof-of-concept study, Antivir. Res. 167 (2019) 83–88, https://doi.org/10.1016/j.antiviral.2019.04.007.
[145] P.K. Prathipati, S. Mandal, G. Pon, R. Vivekanandan, C.J. Destache, Pharmacokinetic and tissue distribution profile of long acting tenofovir alafenamide and elvitegravir loaded nanoparticles in humanized mice model, Pharm. Res. 34 (2017) 2749–2755, https://doi.org/10.1007/s11095-017-2255-7.
[146] What is Pre Exposure Prophylaxis (PrEP), https://www.avert.org/hiv-transmission-prevention/prep, (2020) , Accessed date: 13 April 2020.
[147] A. Attama, M. Momoh, P. Builders, Lipid nanoparticulate drug delivery systems: a revolution in dosage form design and development, Recent Adv. Nov. Drug Carr. Syst. (2012) 107–140.
[148] H. Raina, S. Kaur, A.B. Jindal, Development of efavirenz loaded solid lipid nanoparticles: Risk assessment, quality-by-design (QbD) based optimisation and physicochemical characterisation, J. Drug Deliv. Sci. Technol. 39 (2017) 180–191, https://doi.org/10.1016/j.jddst.2017.02.013.
[149] D.H. Surve, A.B. Jindal, Development and validation of reverse-phase high-performance liquid chromatographic (RP-HPLC) method for quantification of Efavirenz in Efavirenz-Enfuvirtide co-loaded polymer-lipid hybrid nanoparticles, J. Pharm. Biomed. Anal. 175 (2019) 112765, https://doi.org/10.1016/j.jpba.2019.07.013.
[150] M.W. Kim, S. Kwon, J.H. Choi, A. Lee, A promising biocompatible platform: lipid-based and bio-inspired smart drug delivery systems for cancer therapy, Int. J. Mol. Sci. 19 (2018) 1–20, https://doi.org/10.3390/ijms19123859.
[151] A. Laine, J. Gravier, M. Henry, L. Sancey, J. Béjaud, E. Pancani, M. Wiber, I. Texier, J. Coll, J. Benoit, C. Passirani, Conventional versus stealth lipid nanoparticles: Formulation and in vivo fate prediction through FRET monitoring, J. Control. Release 188 (2014) 1–8, https://doi.org/10.1016/j.jconrel.2014.05.042.
[152] A.B. Jindal, S.S. Bachhav, P.V. Devarajan, In situ hybrid nano drug delivery system (IHN-DDS) of antiretroviral drug for simultaneous targeting to multiple viral reservoirs: An in vivo proof of concept, Int. J. Pharm. 521 (2017) 196–203, https://doi.org/10.1016/j.ijpharm.2017.02.024.
[153] P.V. Devarajan, A.B. Jindal, R.R. Patil, F. Mulla, R.V. Gaikwad, A. Samad, Particle shape: a new design parameter for passive targeting in splenotropic drug delivery, J. Pharm. Sci. 99 (2010) 2576–2581, https://doi.org/10.1002/jps.
[154] A.B. Jindal, Nanocarriers for spleen targeting: anatomo-physiological considerations, formulation strategies and therapeutic potential, Drug Deliv. Transl. Res. 6 (2016) 473–485, https://doi.org/10.1007/s13346-016-0304-0.
[155] A.B. Jindal, The effect of particle shape on cellular interaction and drug delivery applications of micro- and nanoparticles, Int. J. Pharm. 532 (2017) 450–465, https://doi.org/10.1016/j.ijpharm.2017.09.028.
[156] J.A. Champion, S. Mitragotri, Role of target geometry in phagocytosis, Proc. Natl. Acad. Sci. 103 (2006) 4930–4934, https://doi.org/10.1073/pnas.0600997103.
[157] N. Doshi, S. Mitragotri, Macrophages recognize size and shape of their targets, PLoS One 5 (2010) 1–6, https://doi.org/10.1371/journal.pone.0010051.
[158] G. Sharma, D. Valenta, Y. Altman, S. Harvey, H. Xie, M. Samir, J. Smith, Polymer particle shape independently influences binding and internalization by macrophages, J. Control. Release 147 (2010) 408–412, https://doi.org/10.1016/j.jconrel.2010.07.116.Polymer.
[159] P.K. Dash, H.E. Gendelman, U. Roy, S. Balkundi, R.L. Mosley, H.A. Gelbard, J. Mcmillan, S. Gorantla, L.Y. Poluektova, Long-acting NanoART elicits potent antiretroviral and neuroprotective responses in HIV-1 infected humanized mice, AIDS 26 (2014) 2135–2144, https://doi.org/10.1097/QAD.0b013e328357f5ad.Long-acting.
[160] B.D. Kevadiya, B. Ottemann, I.Z. Mukadam, L. Castellanos, K. Sikora, J.R. Hilaire, J. Machhi, J. Herskovitz, D. Soni, M. Hasan, S. Anandakumar, J. Garrison, J. Mcmillan, B. Edagwa, R.L. Mosley, R.W. Vachet, H.E. Gendelman, Rod-shape theranostic nanoparticles facilitate antiretroviral drug biodistribution and activity in human immunodeficiency virus susceptible cells and tissues, Theronostics. 10 (2020) 630–656, https://doi.org/10.7150/thno.39847.
[161] J. McMillan, A. Sclachetka, L. Slack, B. Sillman, B. Lamberty, B. Morsey, S. Callen, N. Gautam, Y. Alnouti, B. Edagwa, H. Gendelman, H. Fox, Pharmacokinetics of a long-acting nanoformulated dolutegravir prodrug in rhesus macaques, Antimicrob. Agents Chemother. 62 (2018) 1–5.
[162] J.J. Hobson, A. Al-khouja, P. Curley, D. Meyers, C. Flexner, M. Siccardi, A. Owen, C.F. Meyers, S.P. Rannard, Semi-solid prodrug nanoparticles for long-acting delivery of water-soluble antiretroviral drugs within combination HIV therapies, Nat. Commun. 10 (2019) 1–10, https://doi.org/10.1038/s41467-019-09354-z.
[163] S.N. Kudalkar, J. Beloor, E. Quijano, K.A. Spasov, W. Lee, J.A. Cisneros, From in silico hit to long-acting late-stage preclinical candidate to combat HIV-1 infection, PNAS PLUS (2017) 1–10, https://doi.org/10.1073/pnas.1717932115.
[164] R. Rajoli, D. Back, S. Rannard, C.F. Meyers, C. Flexner, A. Owen, M. Siccardi, Physiologically-based pharmacokinetic modelling to inform development of

intramuscular long acting nanoformulations for HIV, Clin. Pharmacokinet. 54 (2015) 639–650, https://doi.org/10.1007/s40262-014-0227-1.Physiologically-Based.
[165] R. Rajoli, D. Back, S. Rannard, M.F. CAren, C. Flexner, A. Owen, M. Siccardi, In silico dose prediction for long-acting rilpivirine and cabotegravir administration to children and adolescents, Clin. Pharmacokinet. 57 (2018) 255–266, https://doi.org/10.1007/s40262-017-0557-x.In.
[166] R.K.R. Rajoli, C. Flexner, J. Chiong, A. Owen, R.F. Donnelly, Modelling the intradermal delivery of microneedle array patches for long- acting antiretrovirals using PBPK, Eur. J. Pharm. Biopharm. 144 (2019) 101–109, https://doi.org/10.1016/j.ejpb.2019.09.011.
[167] M. Chetty, T.N. Johnson, S. Polak, F. Salem, K. Doki, A. Rostami-hodjegan, Physiologically based pharmacokinetic modelling to guide drug delivery in older people, Adv. Drug Deliv. Rev. 135 (2018) 85–96, https://doi.org/10.1016/j.addr.2018.08.013.
[168] M. Danhof, E.C.M. De Lange, O.E. Della Pasqua, B.A. Ploeger, R.A. Voskuyl, Mechanism-based pharmacokinetic- pharmacodynamic (PK-PD) modeling in translational drug research, Trends Pharmacol. Sci. 29 (2008) 186–191, https://doi.org/10.1016/j.tips.2008.01.007.
[169] S. Gorantla, E. Makarov, J. Finke-dwyer, A. Castanedo, A. Holguin, C.L. Gebhart, H.E. Gendelman, L. Poluektova, Links between progressive HIV-1 infection of humanized mice and viral neuropathogenesis, Am. J. Pathol. 177 (2010) 2938–2949, https://doi.org/10.2353/ajpath.2010.100536.
[170] S. Mandal, G. Kang, P. Kumar, Y. Zhou, W. Fan, Q. Li, C.J. Destache, Nanoencapsulation introduces long-acting phenomenon to tenofovir alafenamide and emtricitabine drug combination: A comparative pre- exposure prophylaxis e ffi cacy study against HIV-1 vaginal transmission, J. Control. Release 294 (2019) 216–225, https://doi.org/10.1016/j.jconrel.2018.12.027.
[171] J.B. Honeycutt, W.O. Thayer, C.E. Baker, R.M. Ribeiro, S.M. Lada, Y. Cao, M.G. Hudgens, D.D. Richman, J.V. Garcia, C. Hill, L. Alamos, S. Diego, C. Hill, N. Carolina, S. Diego, S. Diego, S. Diego, S. Diego, HIV persistence in tissue macrophages of humanized myeloid only mice during antiretroviral therapy, Nat. Med. 23 (2017) 638–643, https://doi.org/10.1038/nm.4319.HIV.
[172] O. Latinovic, M.S. Moreno, L. Hippler, J. Zapata, R. Redfield, Humanized NSG mouse models of HIV-1 infection and pathogenesis, J. Hum. Virol. Retrovirol. 3 (2016) 87–89, https://doi.org/10.15406/jhvrv.2016.03.00088.
[173] D. Li, M. Rochat, M. Nischang, R. Sutmuller, G. Gers-huber, A. Audige, S. Baenziger, U. Hofer, E. Schlaepfer, S. Regenass, K. Amssoms, B. Stoops, A. Van Cauwenberge, D. Boden, G. Kraus, R.F. Speck, Humanized mice recapitulate key features of HIV-1 infection: a novel concept using long-acting anti- retroviral drugs for treating HIV-1, PLoS One 7 (2012) 1–12, https://doi.org/10.1371/journal.pone.0038853.
[174] B.B. Policicchio, I. Pandrea, C. Apetrei, Animal models for Hiv cure research, Front. Immunol. 7 (2016) 1–15, https://doi.org/10.3389/fimmu.2016.00012.
[175] B.M. Nath, K.E. Schumann, J.D. Boyer, The chimpanzee and other non-human-primate models in HIV-1 vaccine research, Trends Microbiol. 8 (2000) 426–431.
[176] T. Hatziioannou, D. Evans, Animal models for HIV/AIDS research, Nat. Rev. Microbiol. 10 (2012) 852–867, https://doi.org/10.1038/nrmicro2911.Animal.
[177] K. Koen, V. Rompay, Tackling HIV and AIDS: contributions by non-human primate models, Nat. Publ. Gr. 46 (2017) 259–270, https://doi.org/10.1038/laban.1279.
[178] A.J. Hessell, N.L. Haigwood, Animal models in HIV-1 protection and therapy, Curr. Opin. HIV AIDS 10 (2015) 170–176, https://doi.org/10.1097/COH.0000000000000152.Animal.
[179] M. Humbert, R.A. Rasmussen, R. Song, H. Ong, P. Sharma, A.L. Chenine, V.G. Kramer, N.B. Siddappa, W. Xu, J.G. Else, F.J. Novembre, E. Strobert, S.P.O. Neil, R.M. Ruprecht, SHIV-1157i and passaged progeny viruses encoding R5 HIV-1 clade C env cause AIDS in rhesus monkeys, Retroviro. 5 (2008) 1–12, https://doi.org/10.1186/1742-4690-5-94.
[180] R. Paliwal, R.J. Babu, S. Palakurthi, Nanomedicine scale-up technologies: feasibilities and challenges, AAPS PharmSciTech 15 (2014) 1527–1534, https://doi.org/10.1208/s12249-014-0177-9.
[181] N. Desai, Challenges in development of nanoparticle-based therapeutics, J. AAPS 14 (2012) 282–295, https://doi.org/10.1208/s12248-012-9339-4.
[182] P.K. Dash, R. Kaminski, R. Bella, H. Su, S. Mathews, T.M. Ahooyi, C. Chen, P. Mancuso, R. Sariyer, P. Ferrante, M. Donadoni, J.A. Robinson, B. Sillman, Z. Lin, J.R. Hilaire, M. Banoub, M. Elango, N. Gautam, R.L. Mosley, L.Y. Poluektova, J. Mcmillan, A.N. Bade, S. Gorantla, I.K. Sariyer, T.H. Burdo, W. Young, S. Amini, J. Gordon, J.M. Jacobson, B. Edagwa, K. Khalili, H.E. Gendelman, Sequential LASER ART and CRISPR treatments mice, Nat. Commun. 10 (2019) 1–20, https://doi.org/10.1038/s41467-019-10366-y.